Principi della spettroscopia nel vicino infrarosso e applicazioni per studi diagnostici e funzionali

Sergio Fantini

Department of Biomedical Engineering

Tufts University, Medford, Massachusetts, USA

Spettroscopia nel vicino infrarosso

- **Breve introduzione storica**
- **Principi della tecnica per lo studio di tessuti biologici**
- **Ossimetria**
- **Mammografia ottica**
- **Studio funzionale del cervello**

Optical Mammography

1930 1940 1950 1960 1970 1980 1990 2000 2010

- Breast transillumination, M. Cutler, Surg. Gynecol. Obstet. **48**, 721 (1929).
- Diaphanography, C.M.Gros, J. Radiol. Electrol. **53**, 297 (1972).
- Lightscanning, E.Carlsen, Diagn. Imaging **4**, 28 (1982).
- Multicenter study, A. Alveryd *et al.*, Cancer **65**, 1671 (1990).

1990's-2000's:
•Time-resolved methods;
•Broadband spectroscopy;
•Optical tomography;
•Co-registration with US, MRI, CT;
•Photo-acoustics, acousto-optics;
•Fluorescence contrast agents.

Optical Oximetry

1930 1940 1950 1960 1970 1980 1990 2000 2010

- Non-pulsatile oximeter, K.Matthes, Arch. Exp. Pathol. Pharmacol. **176**, 683 (1934).
- Calibrated oximetry, G.A.Millikan, Rev. Sci. Instr. **13**, 434 (1942).
- HP Oximeter, E.B.Merrick *et al.*, Hewlett-Packard J. **28**, 2 (1976).
- Pulse oximetry, I. Yoshiya *et al.*, Med. Biol. Eng. Comput. **18**, 27 (1980).

1990's:
Time-resolved, quantitative, absolute tissue oximetry

Functional Brain Imaging

1930 1940 1950 1960 1970 1980 1990 2000 2010

- Non-Invasive brain study, F. Jöbsis, Science **198**, 1264 (1977).

Functional studies:
•B.Chance *et al.*, PNAS **90**, 3770 (1993);
•Y.Hoshi and M.Tamura, J. Appl. Physiol. **75**, 1842 (1993);
•T.Kato *et al.*, J. Cereb. Blood Flow Metab. **13**, 516 (1993);
•A.Villringer *et al.*, Neurosci. Lett. **154**, 101 (1993).

- Fast optical signal, G. Gratton *et al.*, Psychophysiology **32**, 505 (1995).

2000's:
•Co-registration with fMRI, ERP;
•Modeling of NIRS signals;

Epithelial tissue

Stratified squamous epithelium

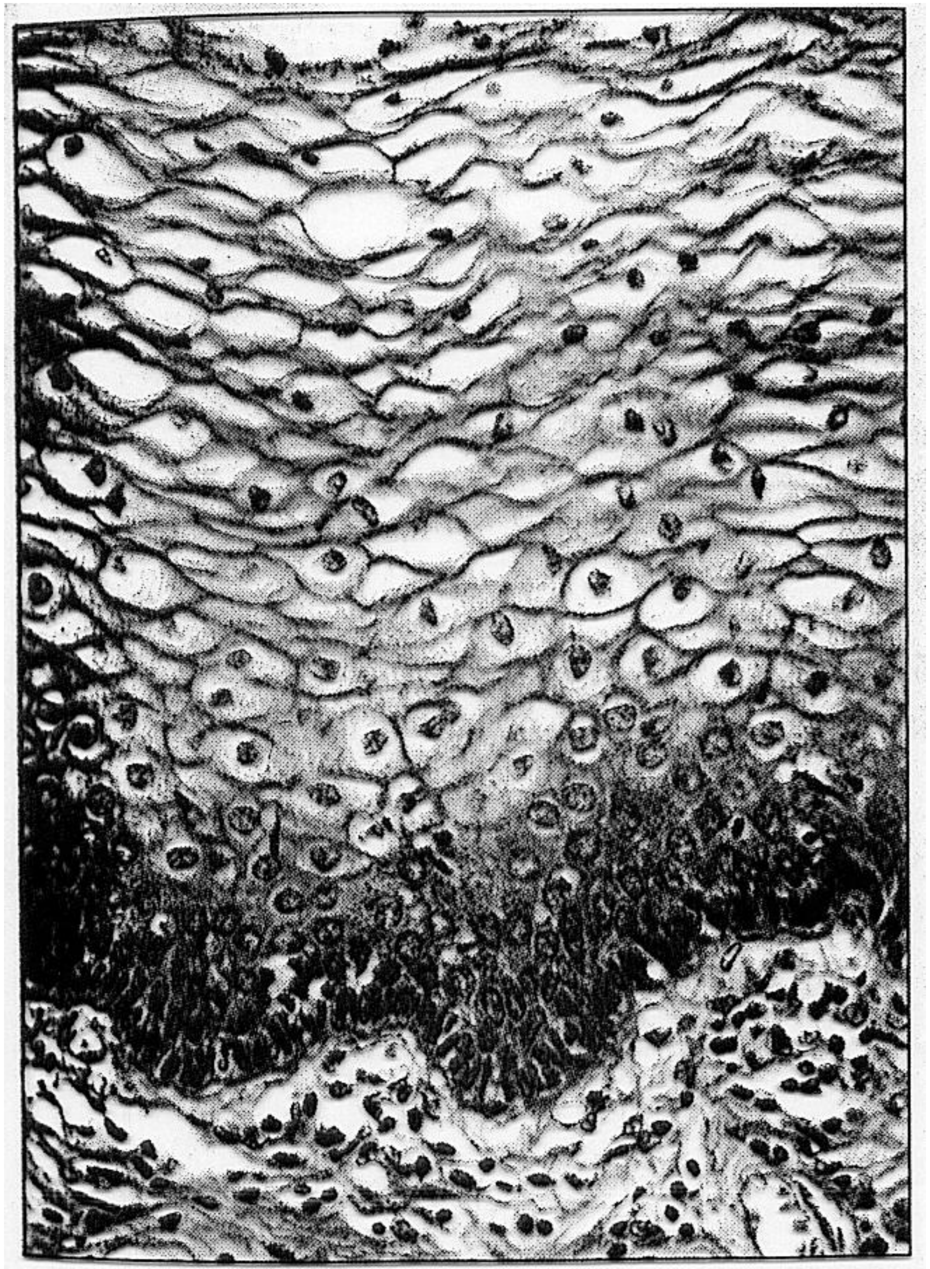

Connective tissue

Loose (areolar) connective tissue

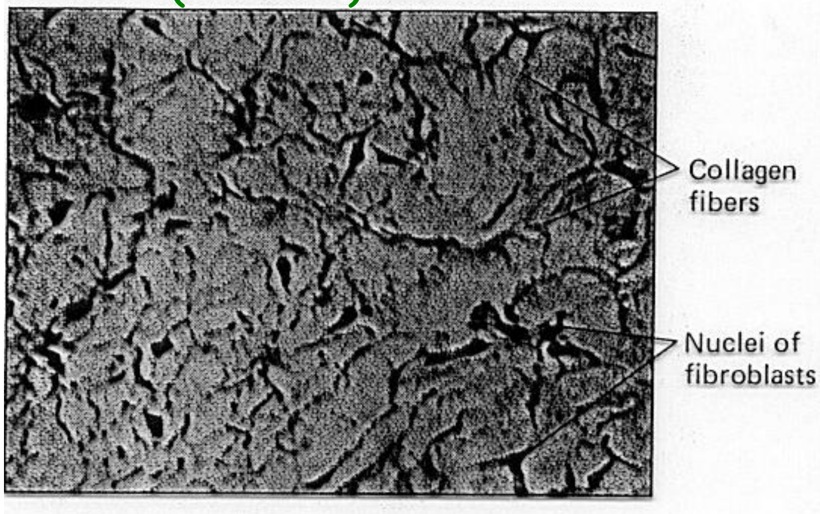

Bone

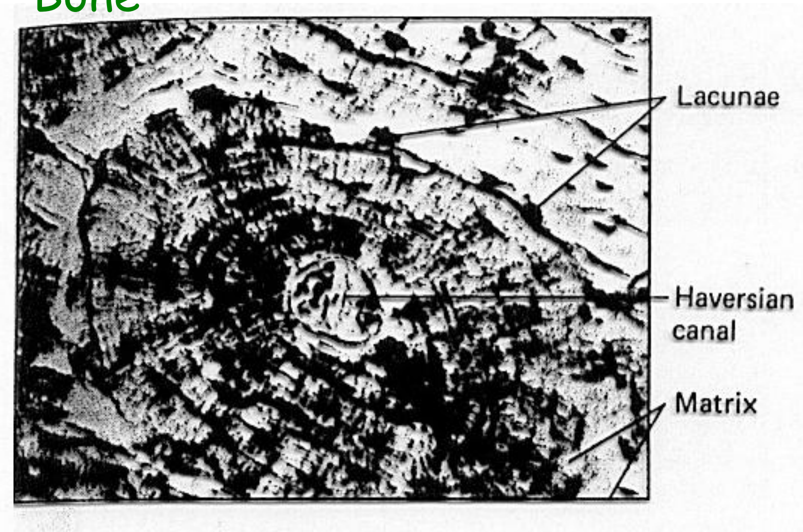

Adipose tissue

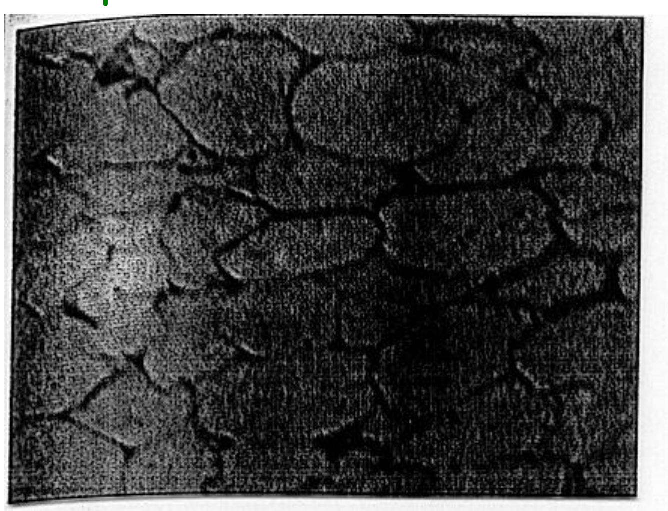

Blood

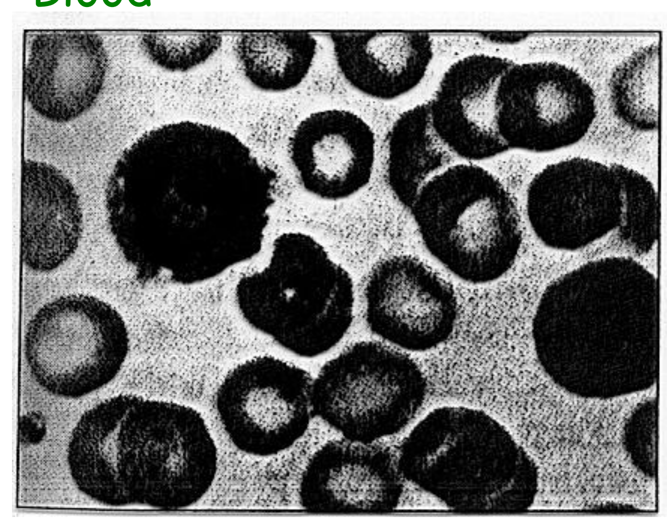

10μm

Muscle tissue

Skeletal muscle

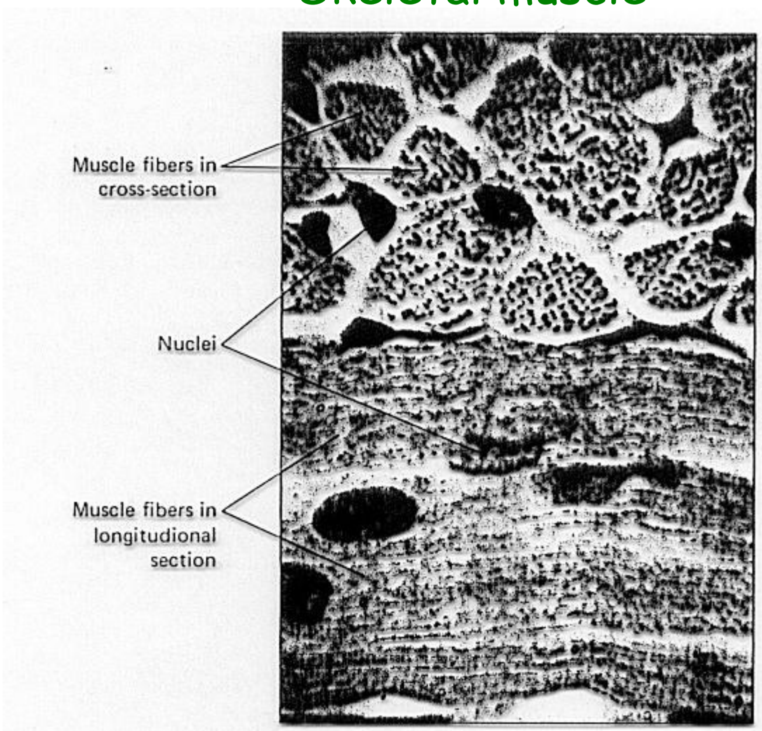

(a)

10µm

Smooth muscle

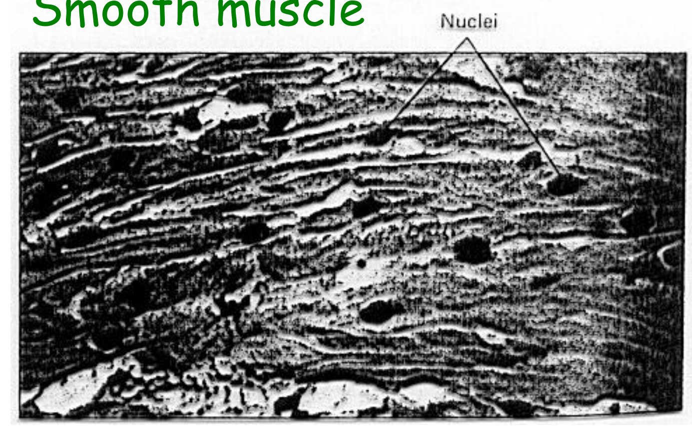

(b)

10µm

Cardiac muscle

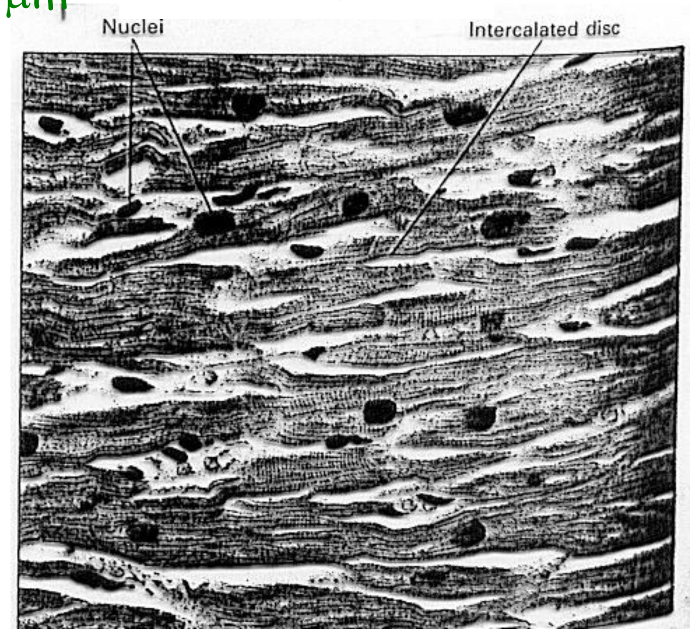

(c)

FIGURE 38–8 Muscle tissue. (*a*) Skeletal muscle is striated, voluntary muscle (magnification approximately ×1000). (*b*) Smooth muscle tissue lacks striations and is involuntary (magnification approximately ×450). (*c*) Cardiac muscle tissue is striated, has branched fibers, and is involuntary. The special junctions between cardiac muscle cells are called intercalated disks.

Generalized animal cell

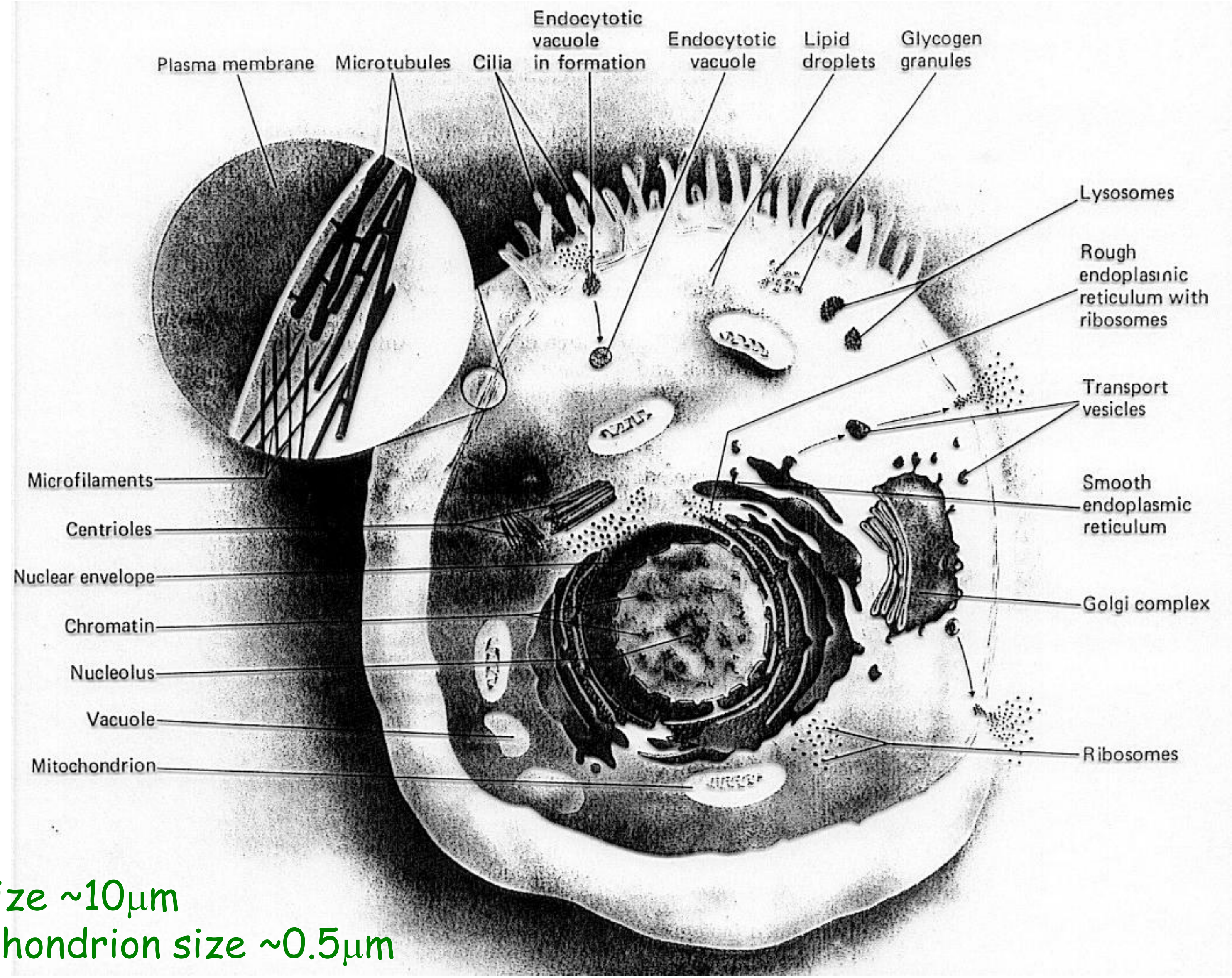

Cell size ~10μm
Mitochondrion size ~0.5μm

Scattering spectra in various tissues

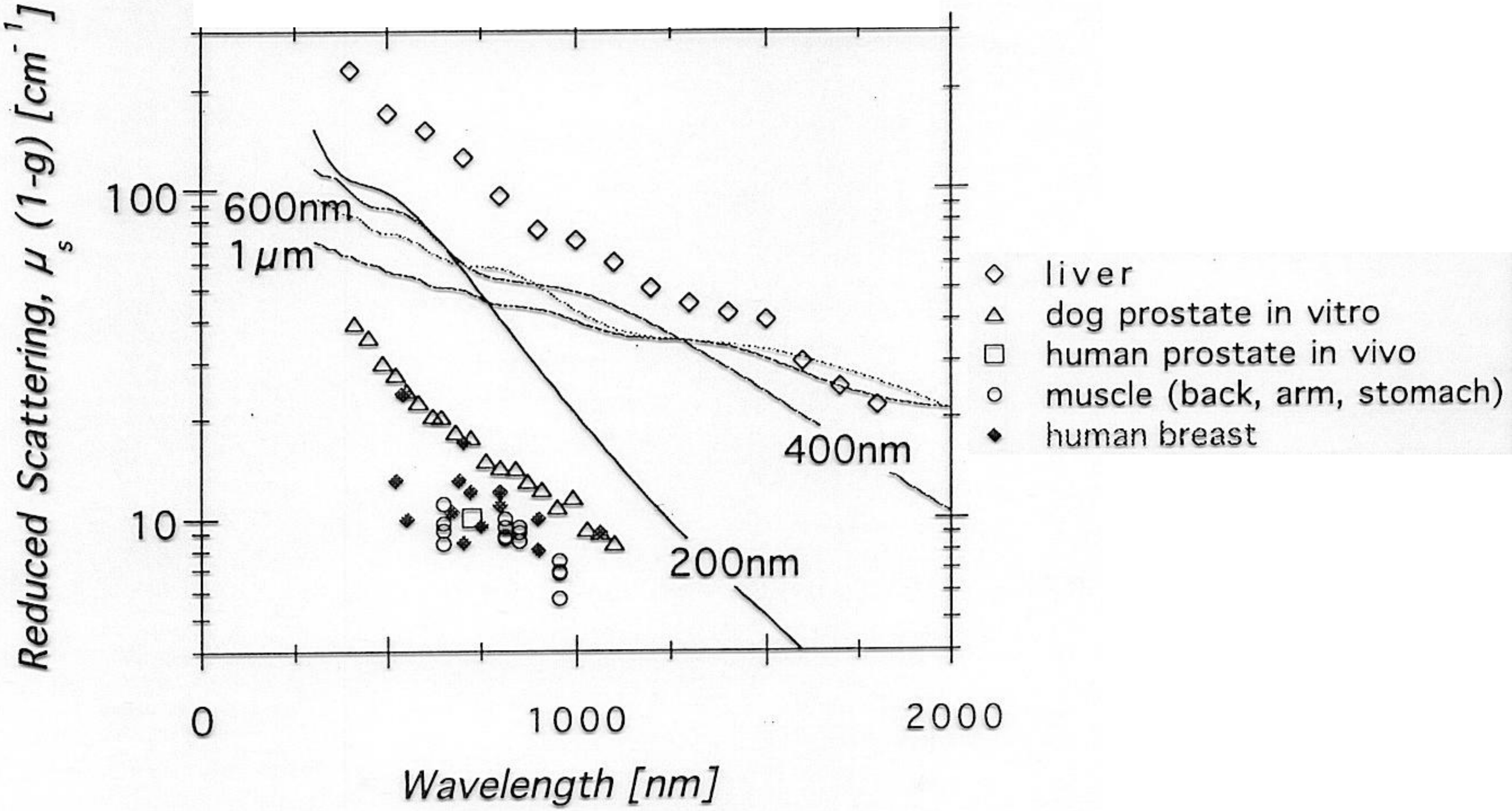

Figure 7. Scattering spectra of tissues (symbols) vs Mie scattering spheres of various diameter (lines). Volume fraction of spheres held constant at 10%.

Glucose effect on the scattering coefficient *in vitro*

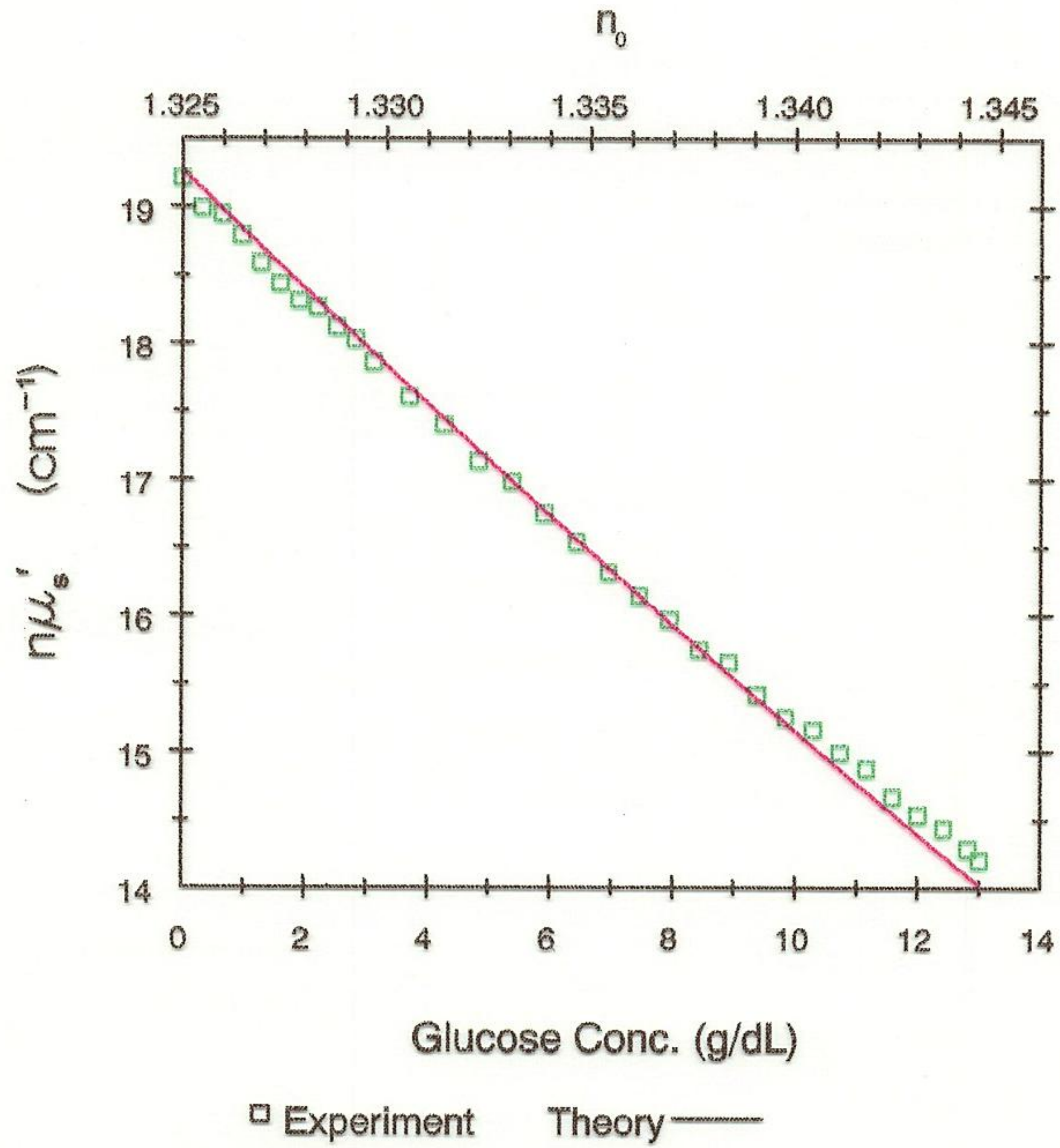

Glucose effect on the scattering coefficient *in vivo*

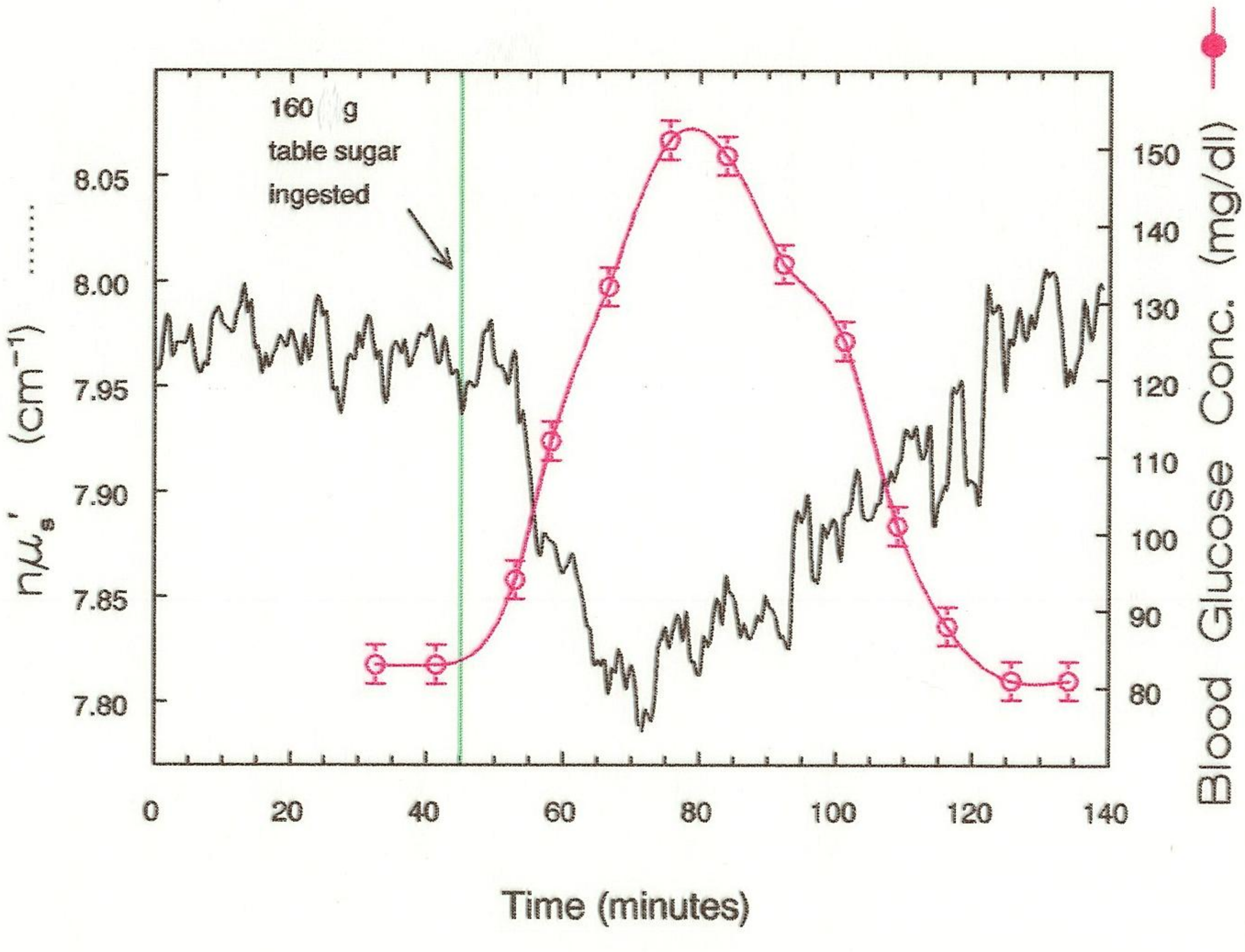

Hemoglobin

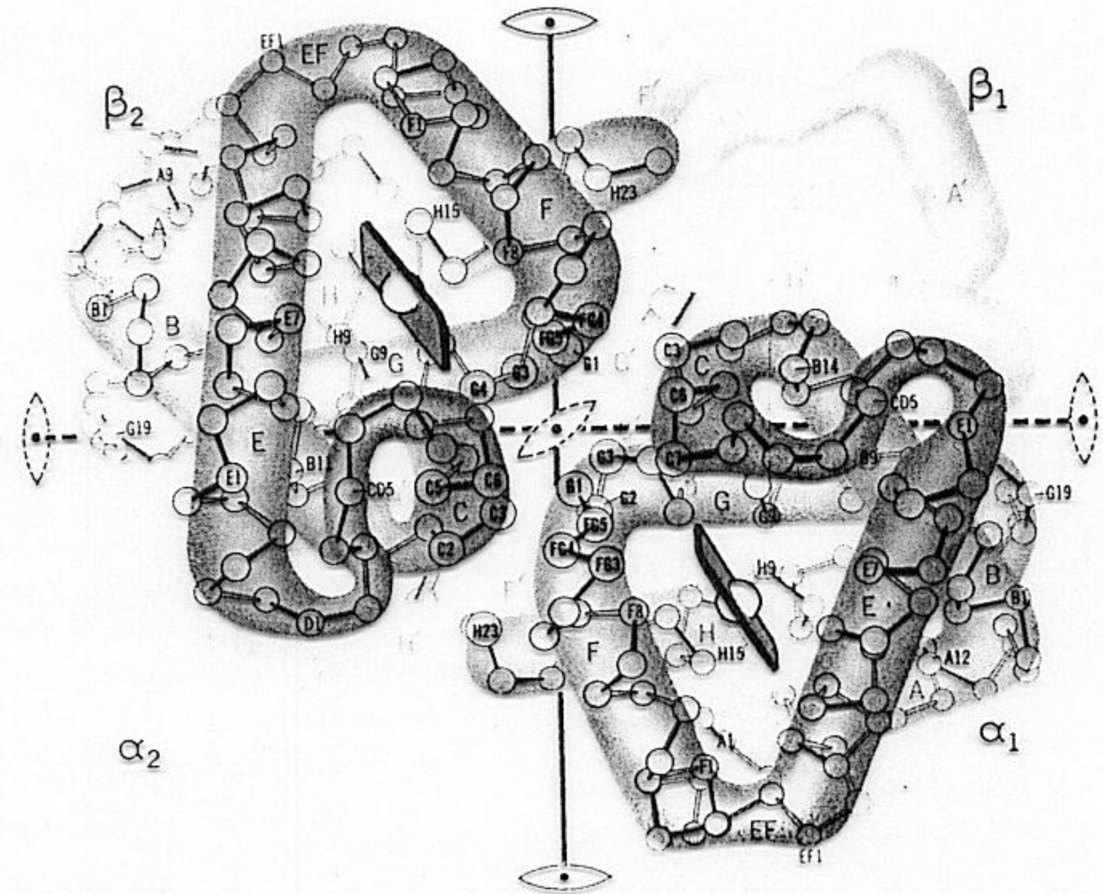

Fig. 2.6. The four chains of oxyhemoglobin (from R. E. Dickerson and I. Geis, *The Structure and Action of Proteins*, W. A. Benjamin Co., Menlo Park. Copyright 1969 Dickerson and Geis)

Hemoglobin absorption spectra

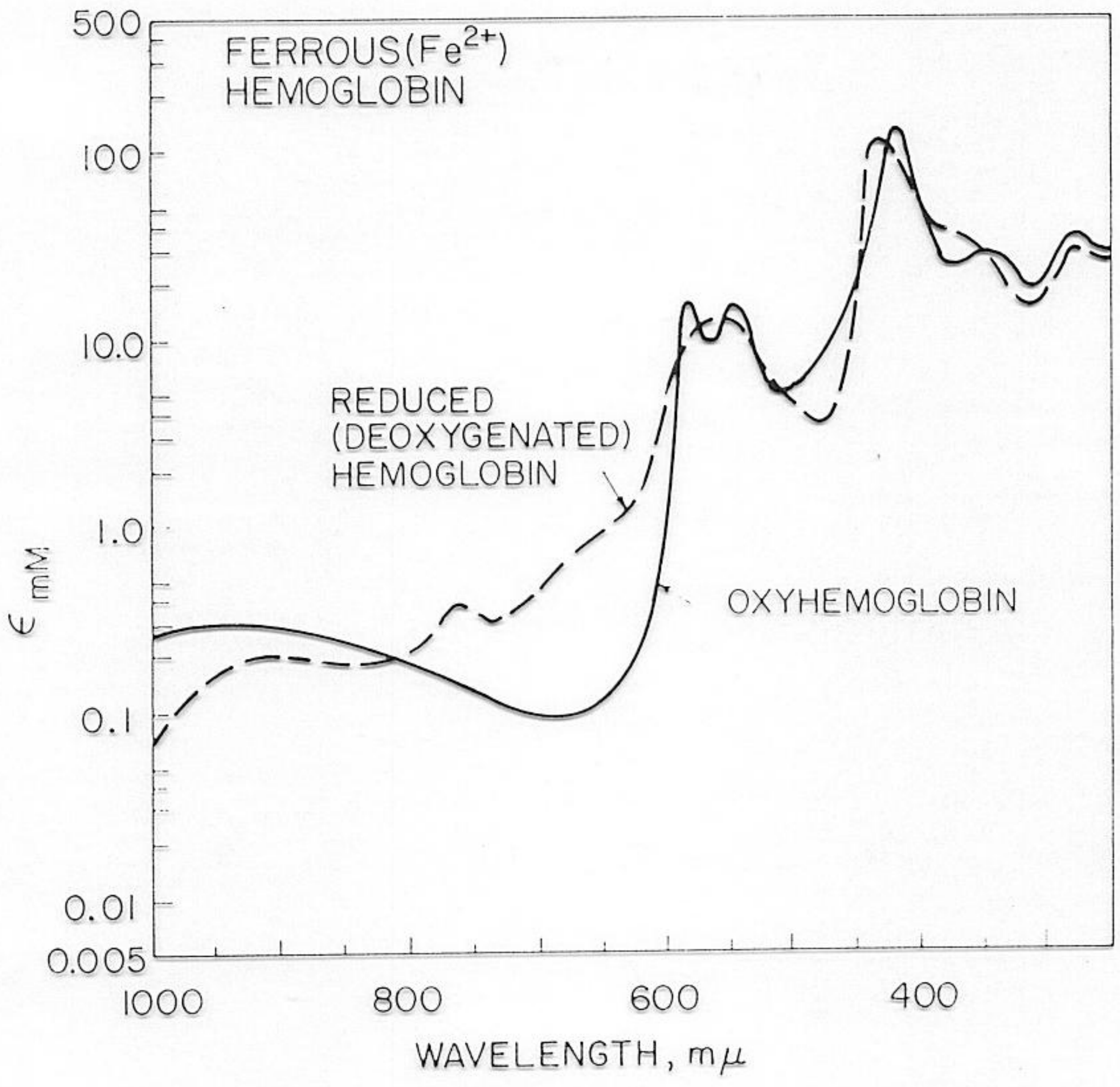

Dominant tissue chromophores in the near infrared

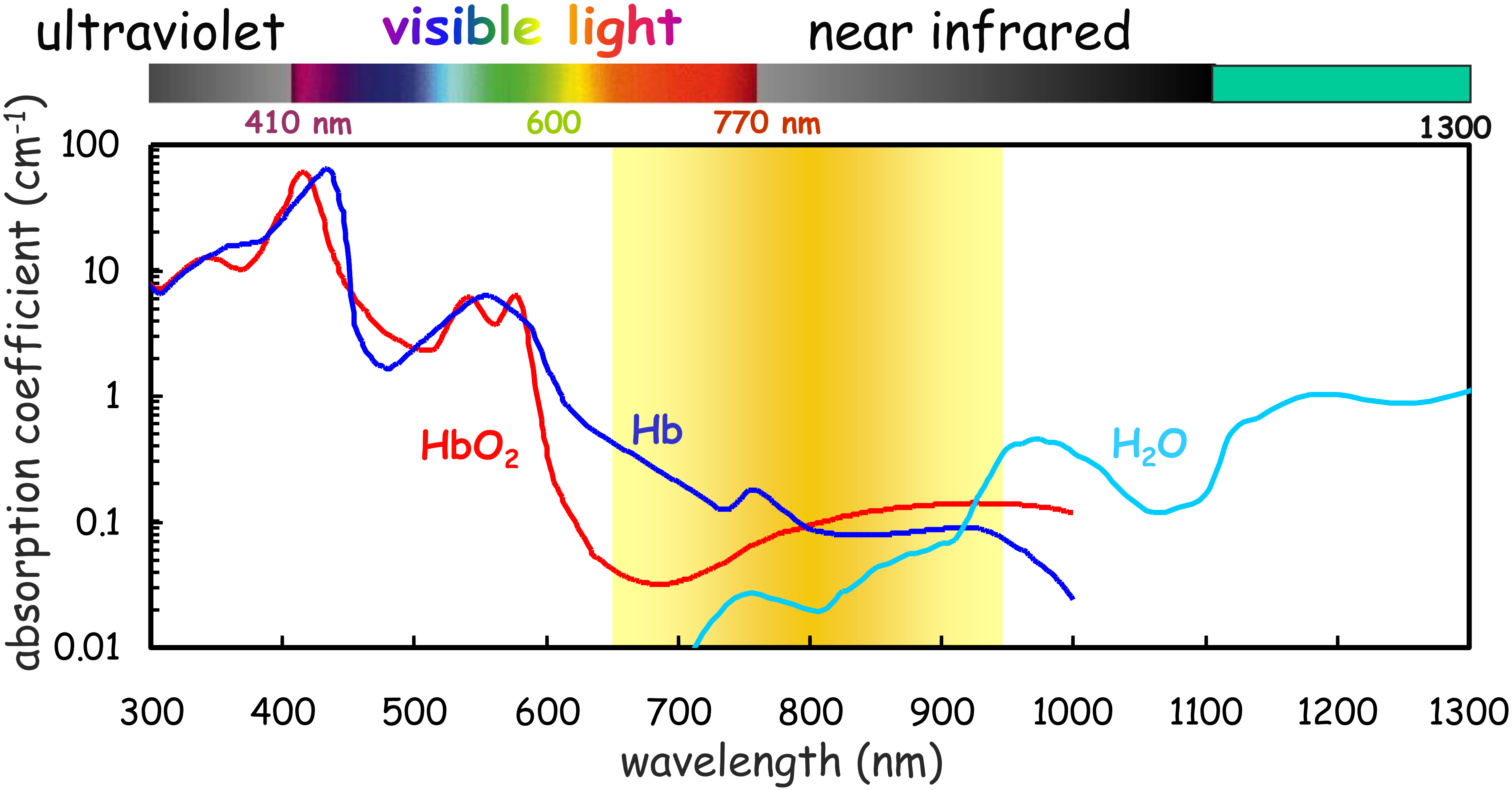

Hb, HbO_2 from: Cheong *et al.*, IEEE J. Quantum Electron. **26**, 2166 (1990)

H_2O from: Hale and Querry, Appl. Opt. **12**, 555 (1973)

Diffusion of near-infrared light inside tissues

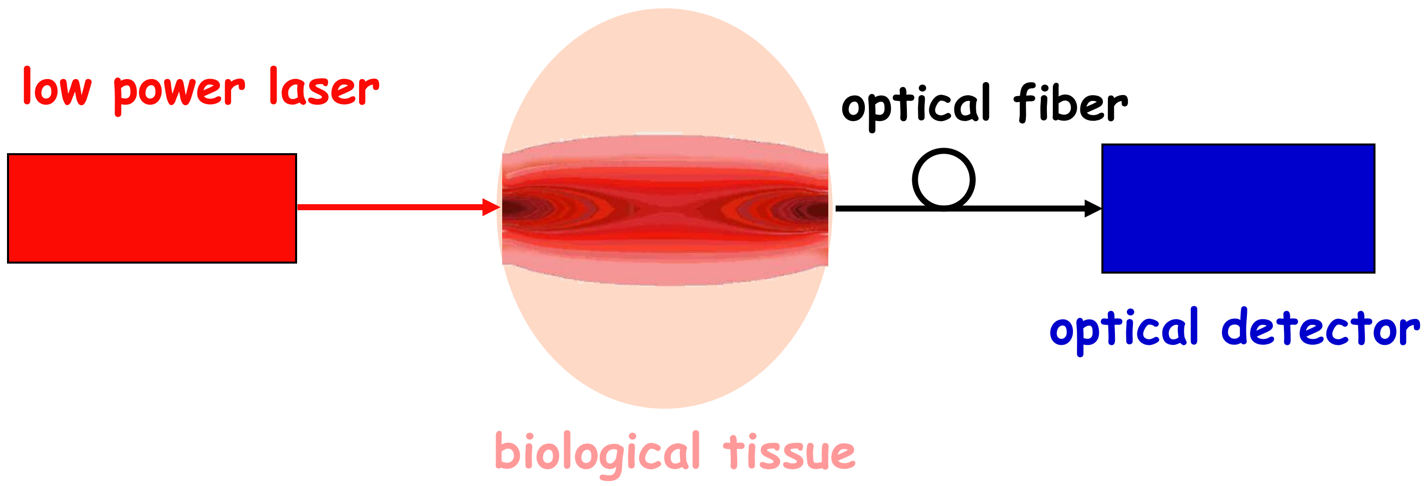

high scattering problem

Experimental approach to tissue spectroscopy

Continuous wave (CW)

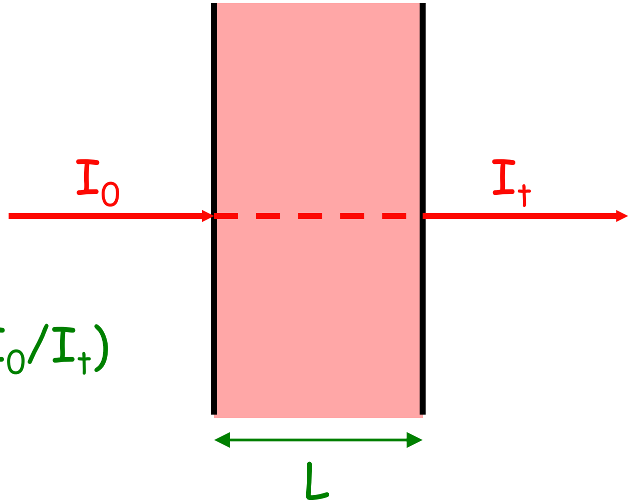

$\mu_a = 1/L \ln(I_0/I_t)$

Time domain (TD)

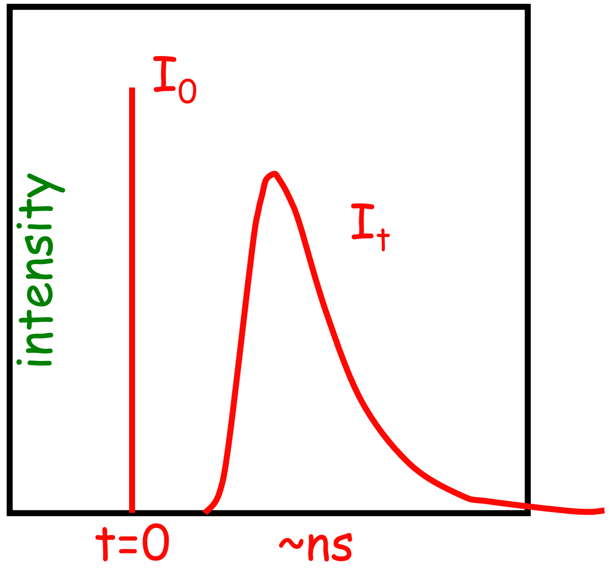

Frequency-domain spectroscopy (FD)

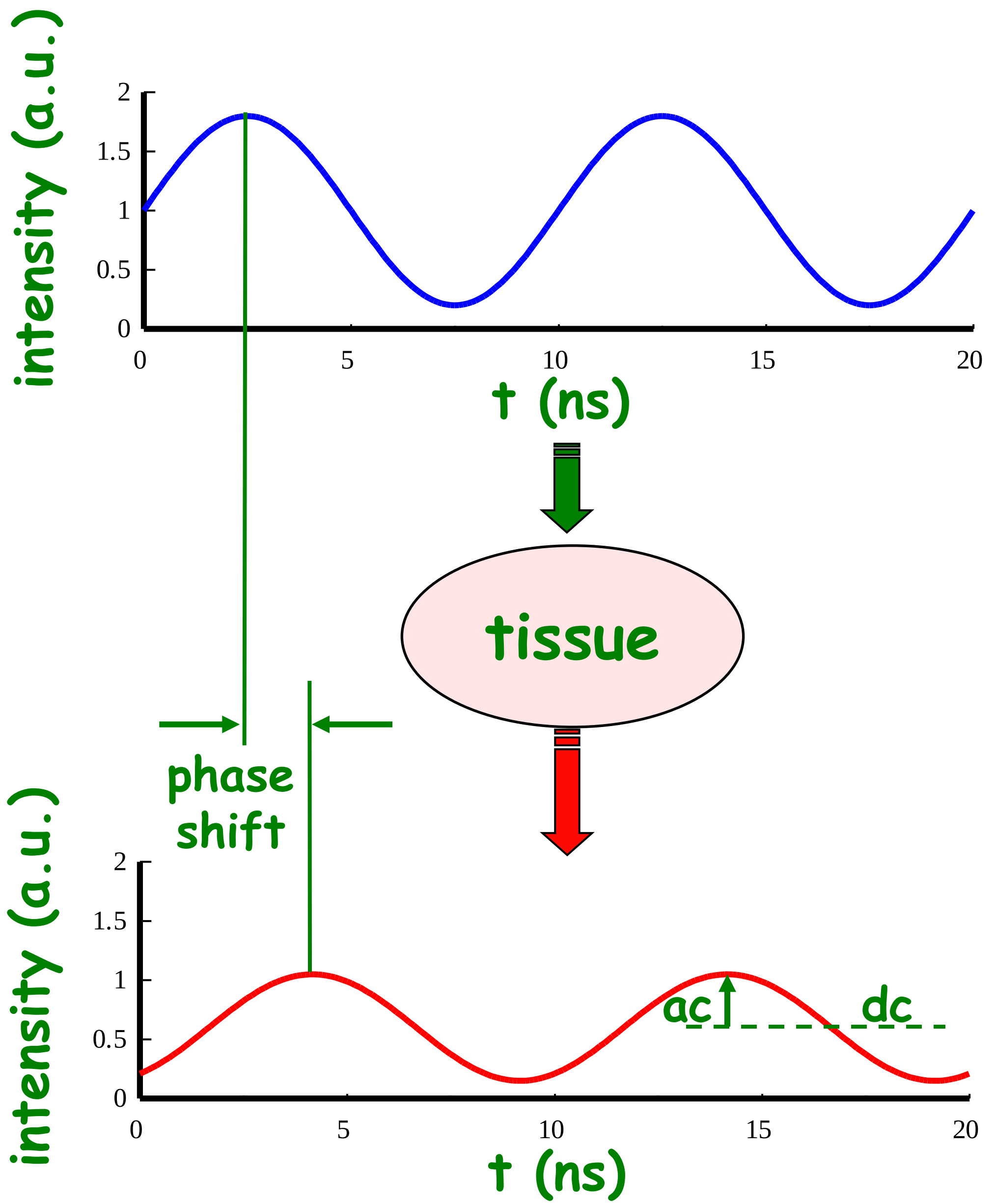

Diffusion equation for the photon density U(r, t)

$$\frac{\partial U(\mathbf{r},t)}{\partial t} - vD\nabla^2 U(\mathbf{r},t) + v\mu_a U(\mathbf{r},t) = q(\mathbf{r},t)$$

$D = 1/[3(\mu_a+\mu_s')]$ = diffusion coefficient

μ_a = absorption coefficient

μ_s' = reduced scattering coefficient

v = speed of light in tissue

q = source term (power per unit volume)

frequency-domain Green's function G(r,ω) for an infinite geometry:

$$G(r,\omega) = \frac{1}{4\pi vD}\frac{e^{-kr}}{r}$$

with $k = \left(\dfrac{v\mu_a - i\omega}{vD}\right)^{1/2}$

Straight lines as a function of r (distance from the source)

from the following definitions:

$Abs[G(r,0)] \equiv$ dc intensity (or average intensity I_{dc})
$Abs[G(r,\omega)] \equiv$ ac amplitude
$Arg[G(r,\omega)] \equiv$ phase

it follows that (for the Green's function):

$\ln(r\, I_{dc}) = -r\, Re[k] - \ln[4\pi v D]$

phase $= r\, Im[k]$

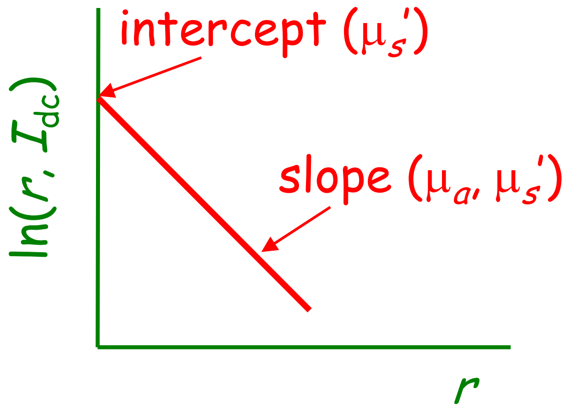

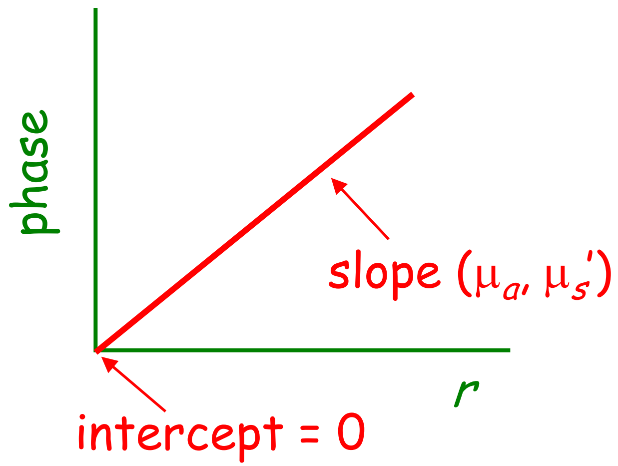

Measurement of absorption and reduced scattering coefficients with frequency-domain spectroscopy

$$\mu_a = \frac{\omega}{2v}\left(\frac{S_\Phi}{S_{ac}} - \frac{S_{ac}}{S_\Phi}\right)$$

$$\mu_s' = \frac{S_{ac}^2 - S_\Phi^2}{3\mu_a} - \mu_a$$

where:

μ_a:	absorption coefficient
μ_s':	reduced scattering coefficient
ω:	angular modulation frequency
v:	speed of light in tissue
S_Φ:	phase slope
S_{ac}:	$\ln(r\,\lvert U_\omega \rvert)$ slope

Translating the absorption coefficient into hemoglobin-related parameters

$$\mu_a(\lambda_i) = \varepsilon_{\mathrm{HbO_2}}(\lambda_i)[\mathrm{HbO_2}] + \varepsilon_{\mathrm{Hb}}(\lambda_i)[\mathrm{Hb}] + \varepsilon_{\mathrm{H_2O}}(\lambda_i)[\mathrm{H_2O}]$$

Oxy-hemoglobin concentration

Deoxy-hemoglobin concentration

$$[\mathrm{HbO_2}] = \frac{\left(\sum_i \mu_a(\lambda_i)\varepsilon_{\mathrm{HbO2}}(\lambda_i)\right)\left(\sum_i \varepsilon^2_{\mathrm{Hb}}(\lambda_i)\right) - \left(\sum_i \mu_a(\lambda_i)\varepsilon_{\mathrm{Hb}}(\lambda_i)\right)\left(\sum_i \varepsilon_{\mathrm{HbO2}}(\lambda_i)\varepsilon_{\mathrm{Hb}}(\lambda_i)\right)}{\left(\sum_i \varepsilon^2_{\mathrm{HbO2}}(\lambda_i)\right)\left(\sum_i \varepsilon^2_{\mathrm{Hb}}(\lambda_i)\right) - \left(\sum_i \varepsilon_{\mathrm{HbO2}}(\lambda_i)\varepsilon_{\mathrm{Hb}}(\lambda_i)\right)^2}$$

$$[\mathrm{Hb}] = \frac{\left(\sum_i \mu_a(\lambda_i)\varepsilon_{\mathrm{Hb}}(\lambda_i)\right)\left(\sum_i \varepsilon^2_{\mathrm{HbO2}}(\lambda_i)\right) - \left(\sum_i \mu_a(\lambda_i)\varepsilon_{\mathrm{HbO2}}(\lambda_i)\right)\left(\sum_i \varepsilon_{\mathrm{HbO2}}(\lambda_i)\varepsilon_{\mathrm{Hb}}(\lambda_i)\right)}{\left(\sum_i \varepsilon^2_{\mathrm{HbO2}}(\lambda_i)\right)\left(\sum_i \varepsilon^2_{\mathrm{Hb}}(\lambda_i)\right) - \left(\sum_i \varepsilon_{\mathrm{HbO2}}(\lambda_i)\varepsilon_{\mathrm{Hb}}(\lambda_i)\right)^2}$$

$$THC = [\mathrm{Hb}] + [\mathrm{HbO_2}]$$

Total hemoglobin concentration

$$\mathrm{StO_2} = \frac{[\mathrm{HbO_2}]}{[\mathrm{Hb}] + [\mathrm{HbO_2}]}$$

Hemoglobin saturation (Y)

TISSUE OXIMETRY

Configuration for tissue oximetry

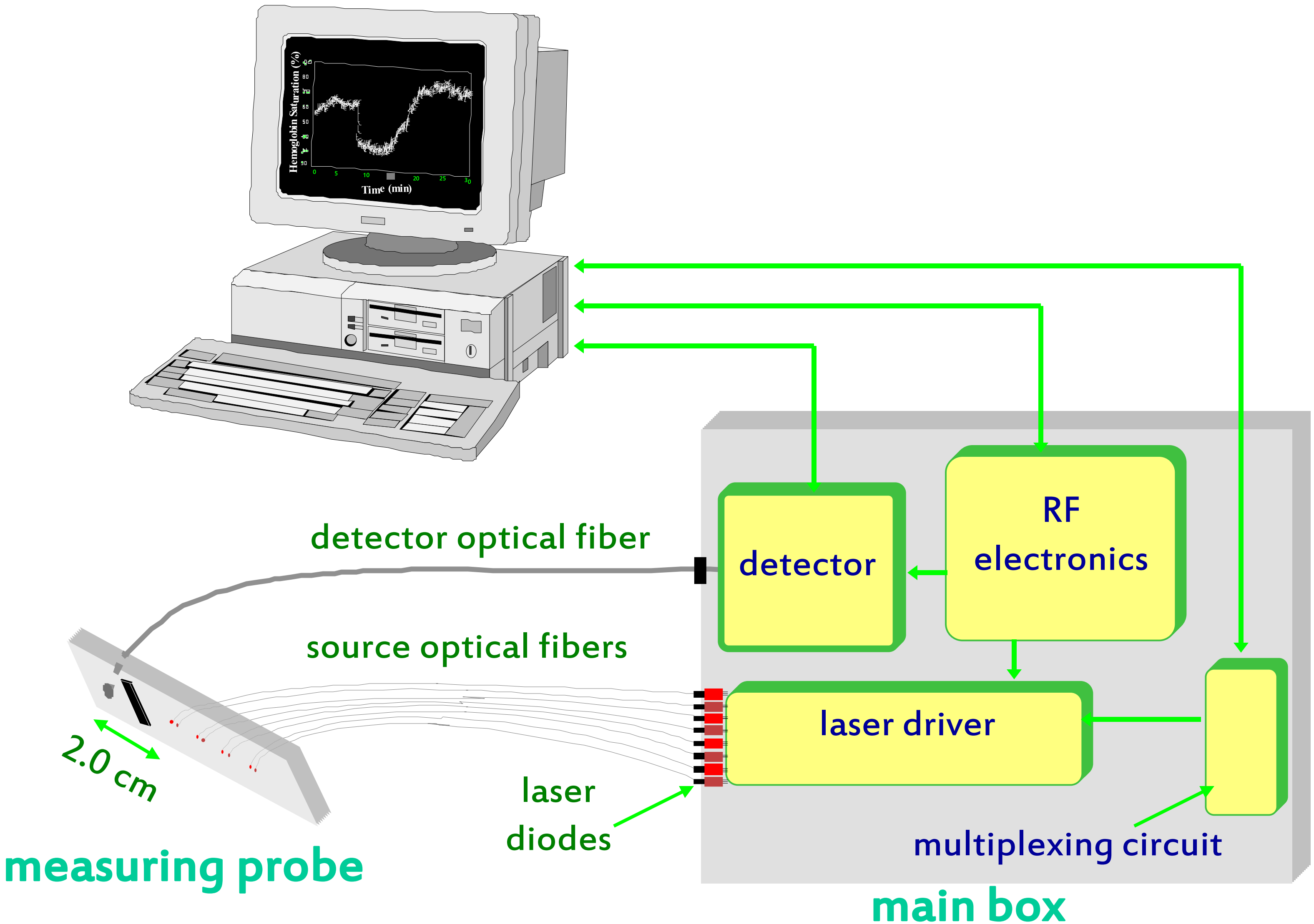

OxiplexTS, ISS, Inc., Champaign, Illinois

Frequency-domain oximetry

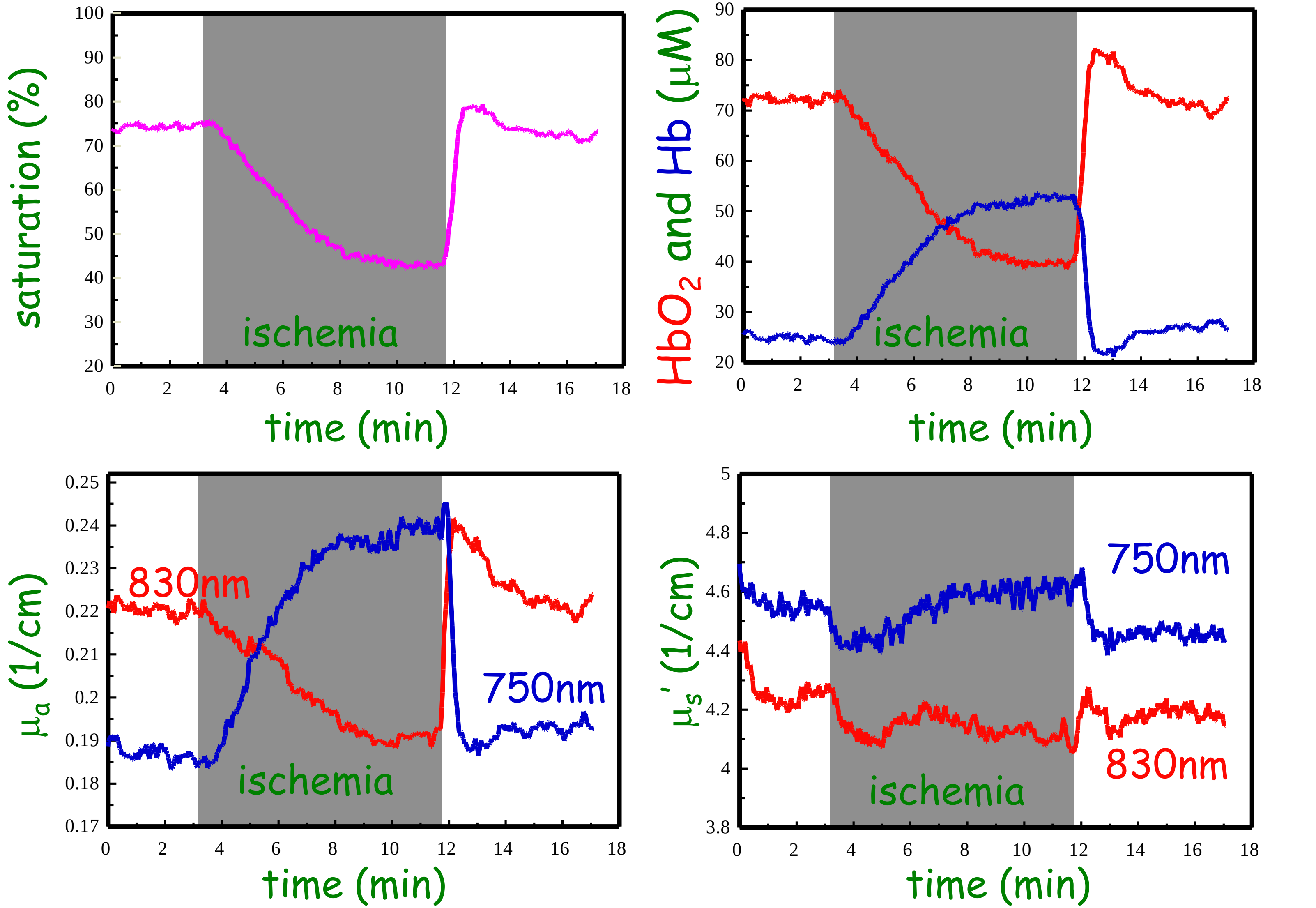

Arterial occlusion → oxygen consumption

(measurement on the forearm of subject 1)

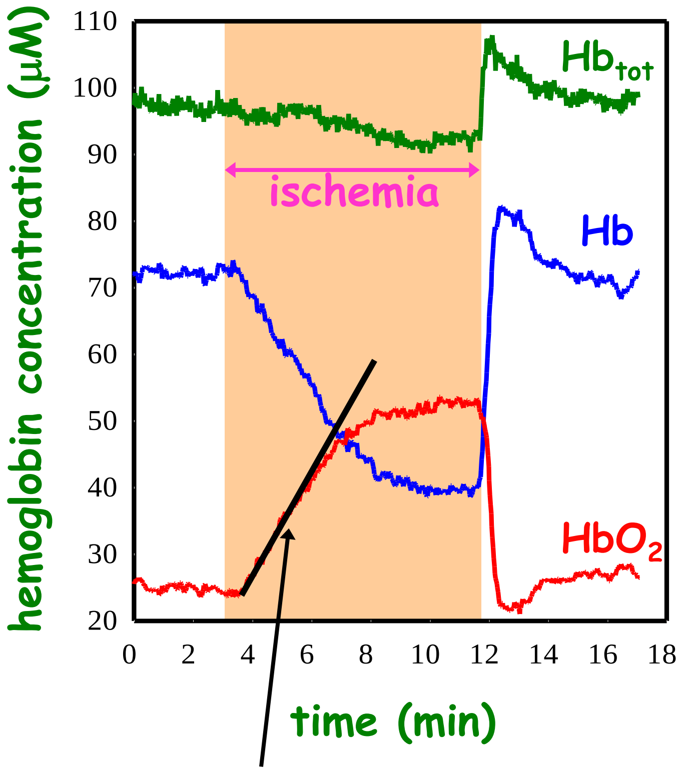

oxygen consumption = 3.2 μmol/100mL/min

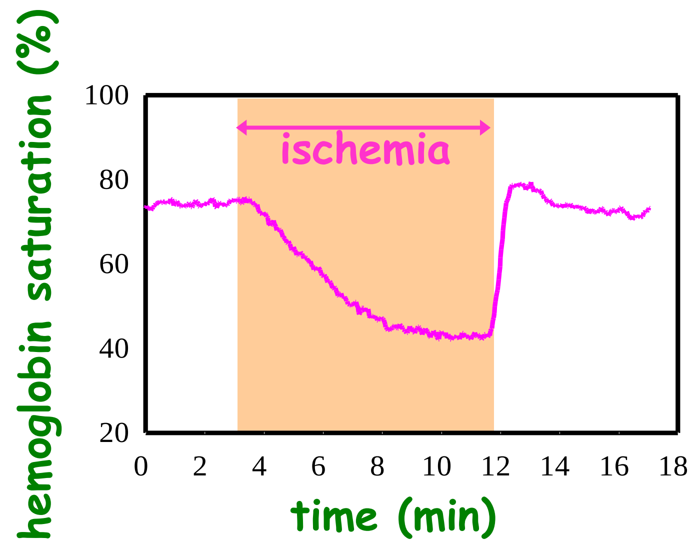

Venous occlusion → blood flow

(measurement on the forearm of subject 2)

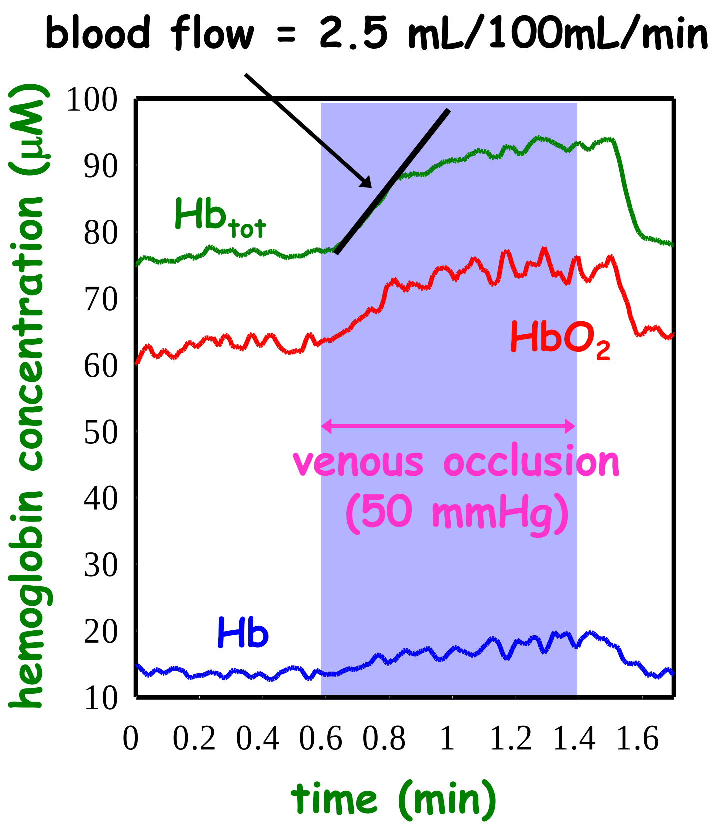

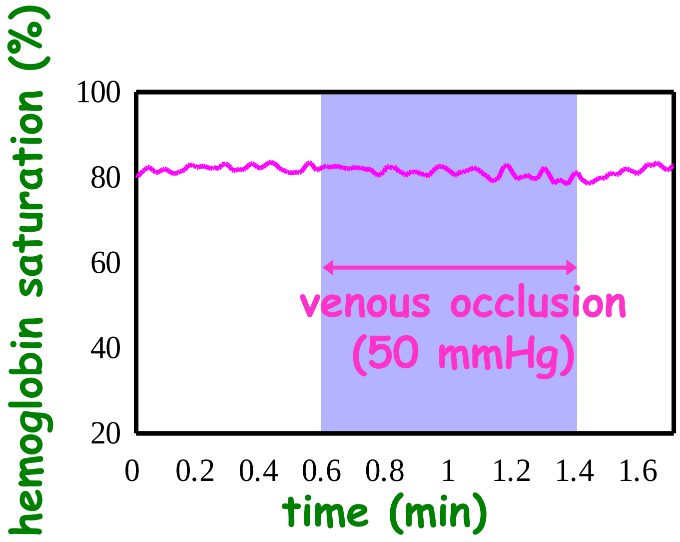

Measurement on the forehead at different percentages of inspired oxygen

probe geometry

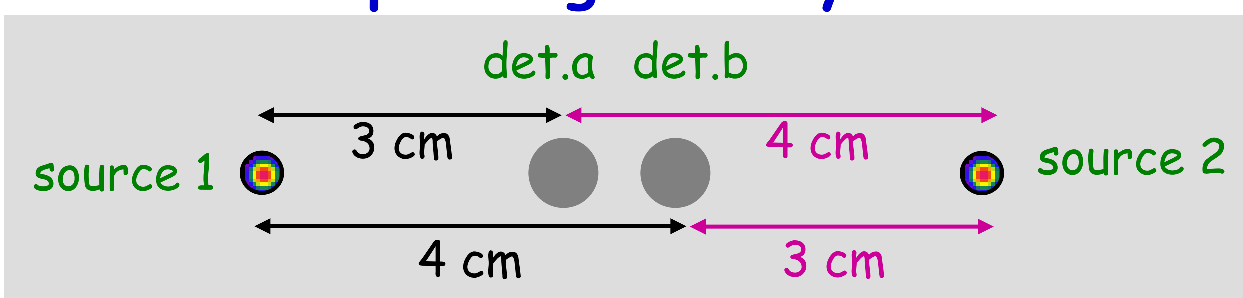

Absorption spectra of the forehead at different inspired oxygen concentrations

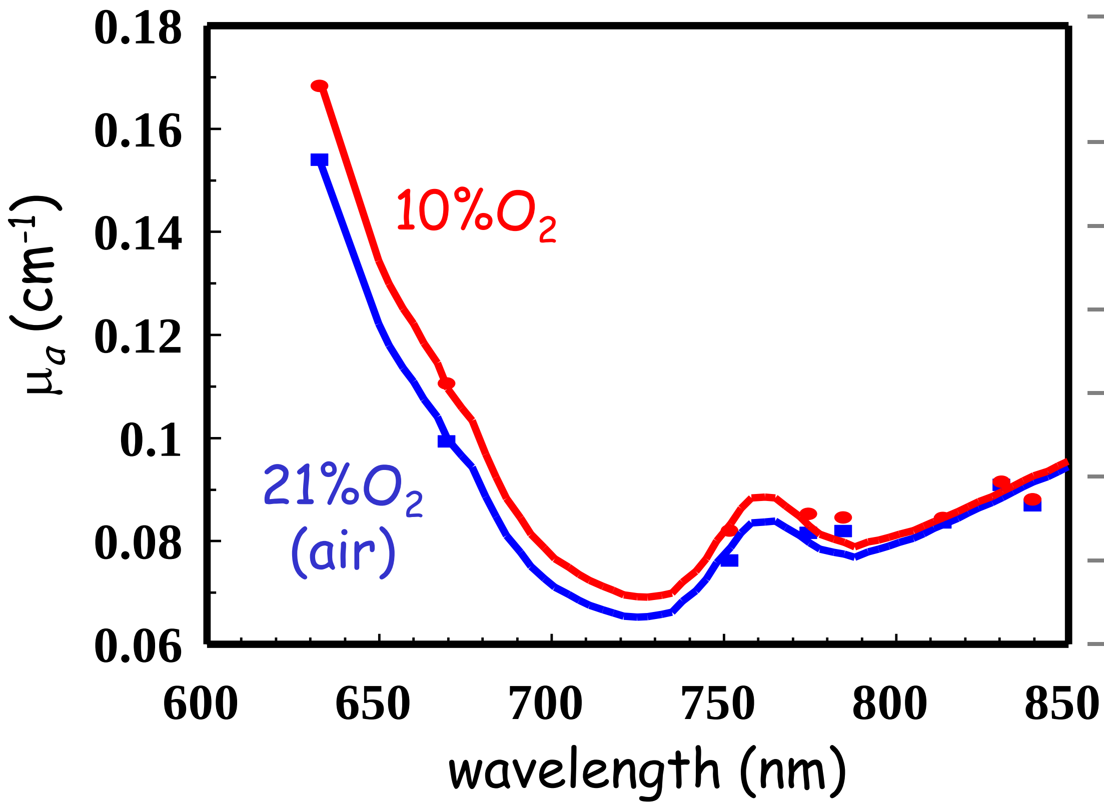

	21% O_2	after 1 min of 10% O_2	
HbO_2	30.2	29.5	μM
Hb	10.1	11.6	μM
THC	40.3	41.2	μM
Y	74.9	71.8	%
SaO_2	97	93	%
pulse	85	86	beat/min

Arterial pulse and absorption coefficient

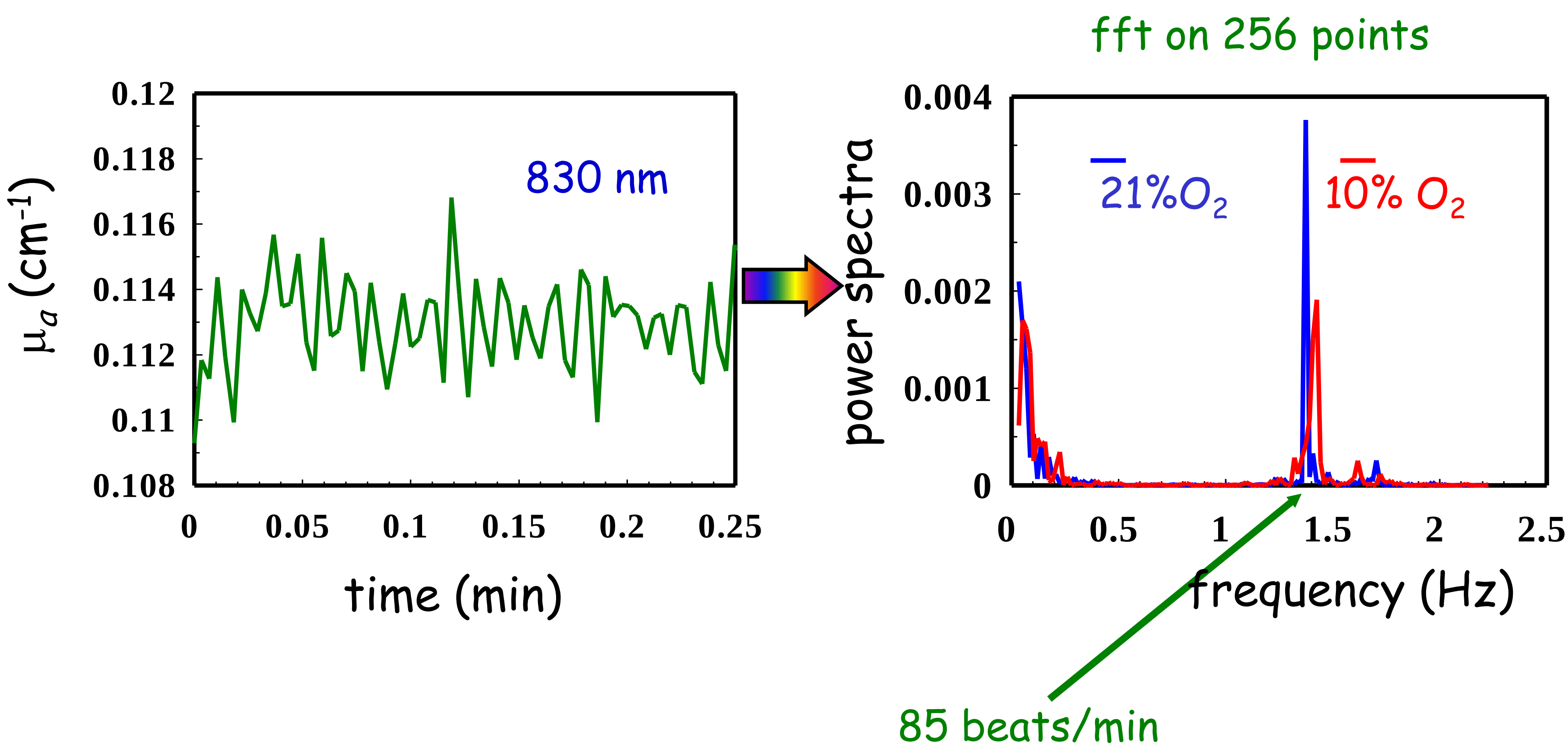

Arterial saturation from pulsatile $\Delta\mu_a$ absorption

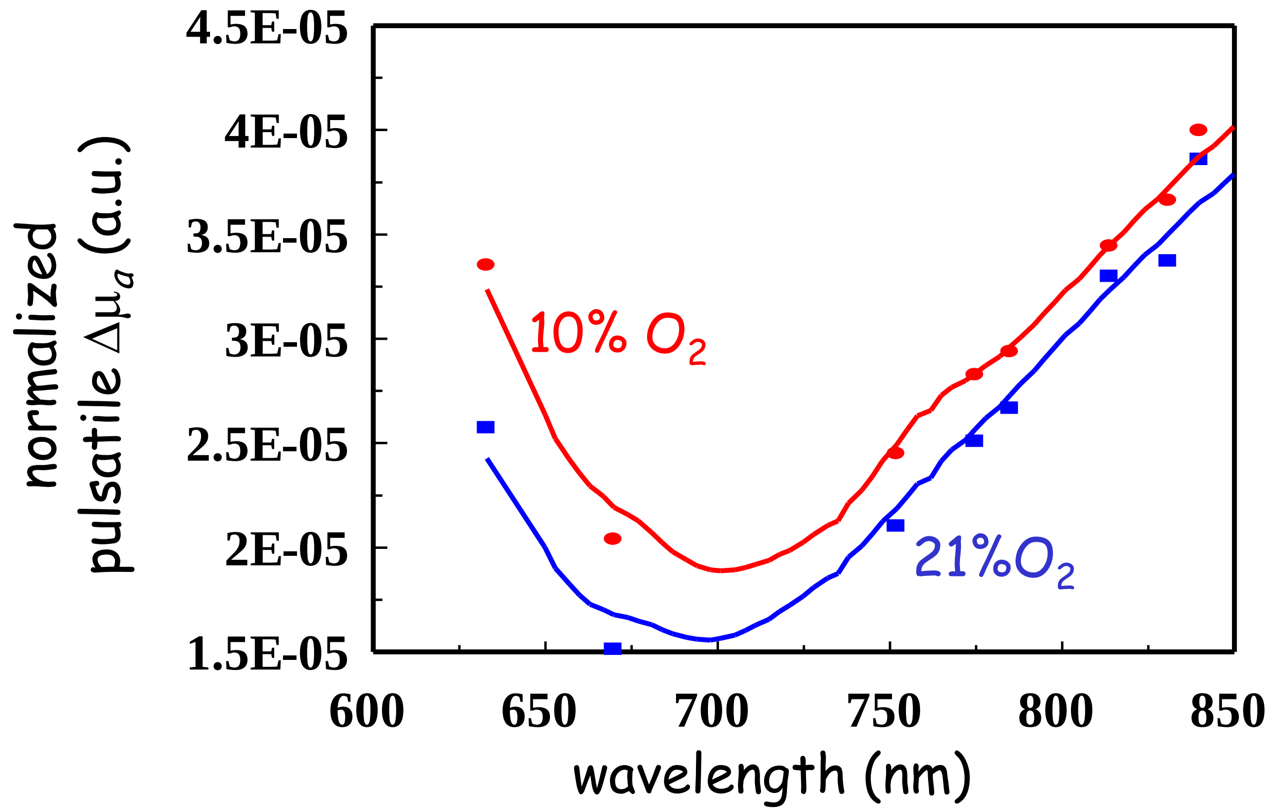

	$21\%O_2$	$10\%O_2$	
SaO_2 with tissue spectrometer	98	94	%
SaO_2 with pulse oximeter	97	93	%

Tissue and arterial saturation

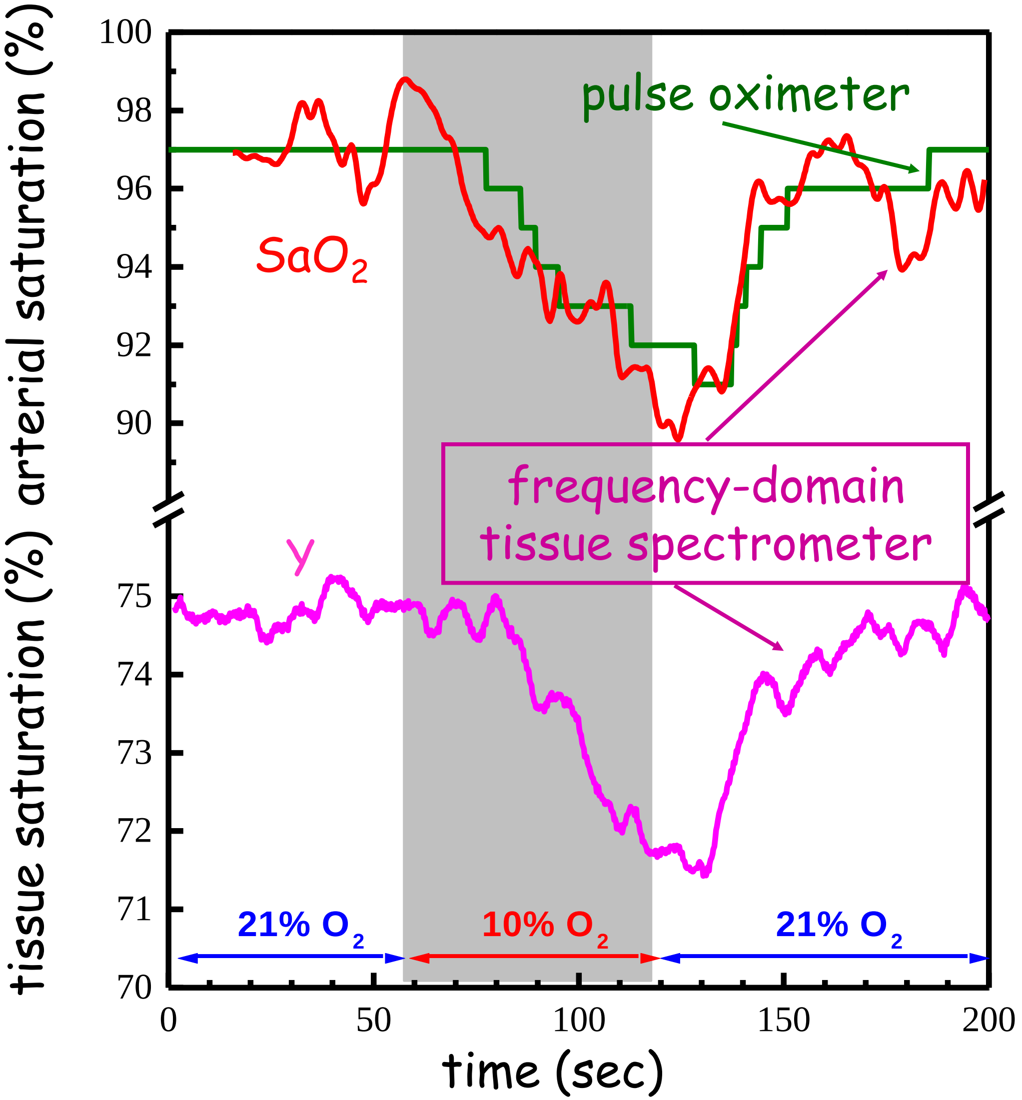

OPTICAL MAMMOGRAPHY

The first optical study of the breast: 1929

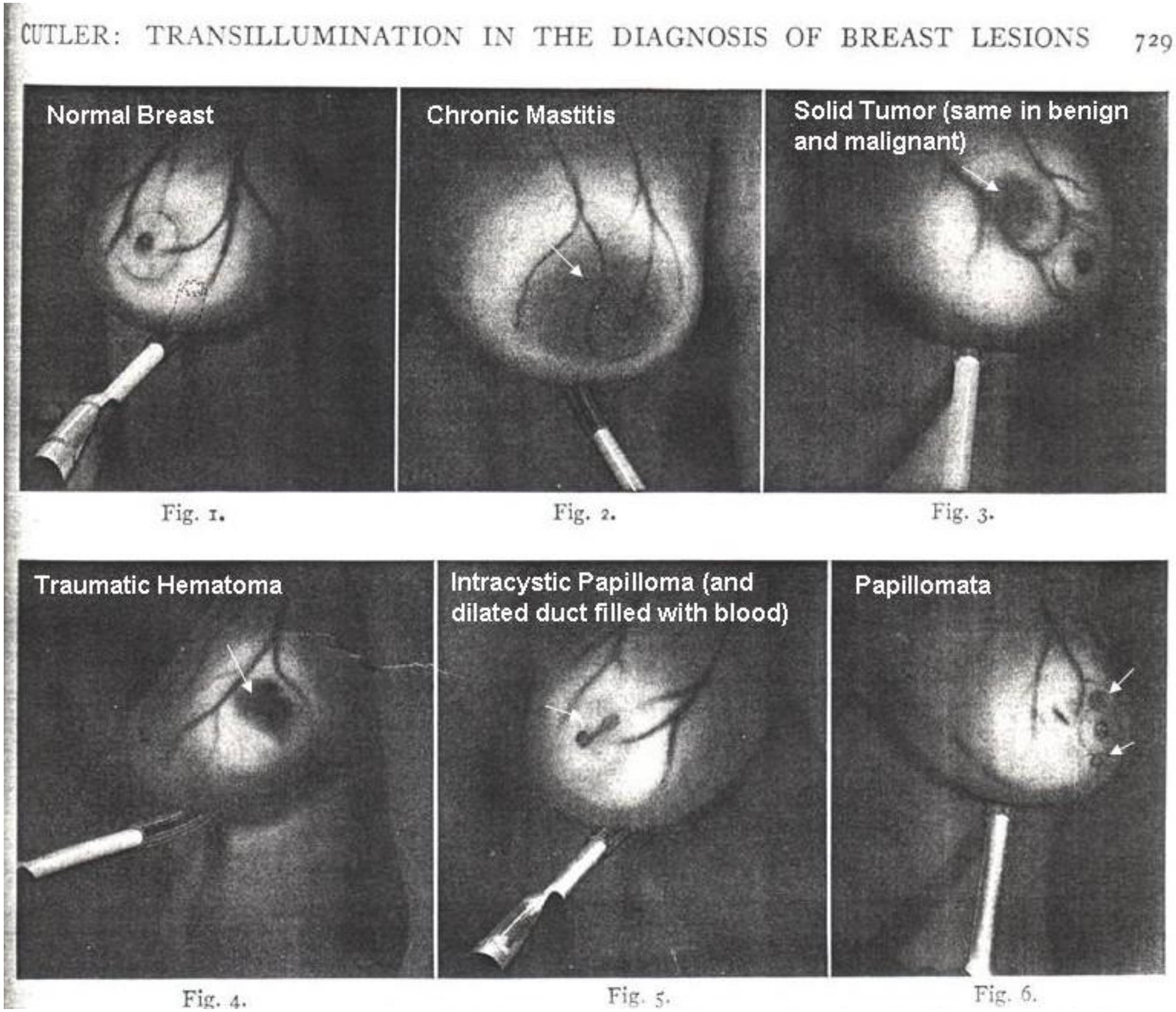

M. Cutler, "Transillumination of the Breast," Surg. Gynecol. Obstet. **48**, 721-727 (1929). (now J. Am. Coll. Surg.)

instrument for frequency-domain optical mammography

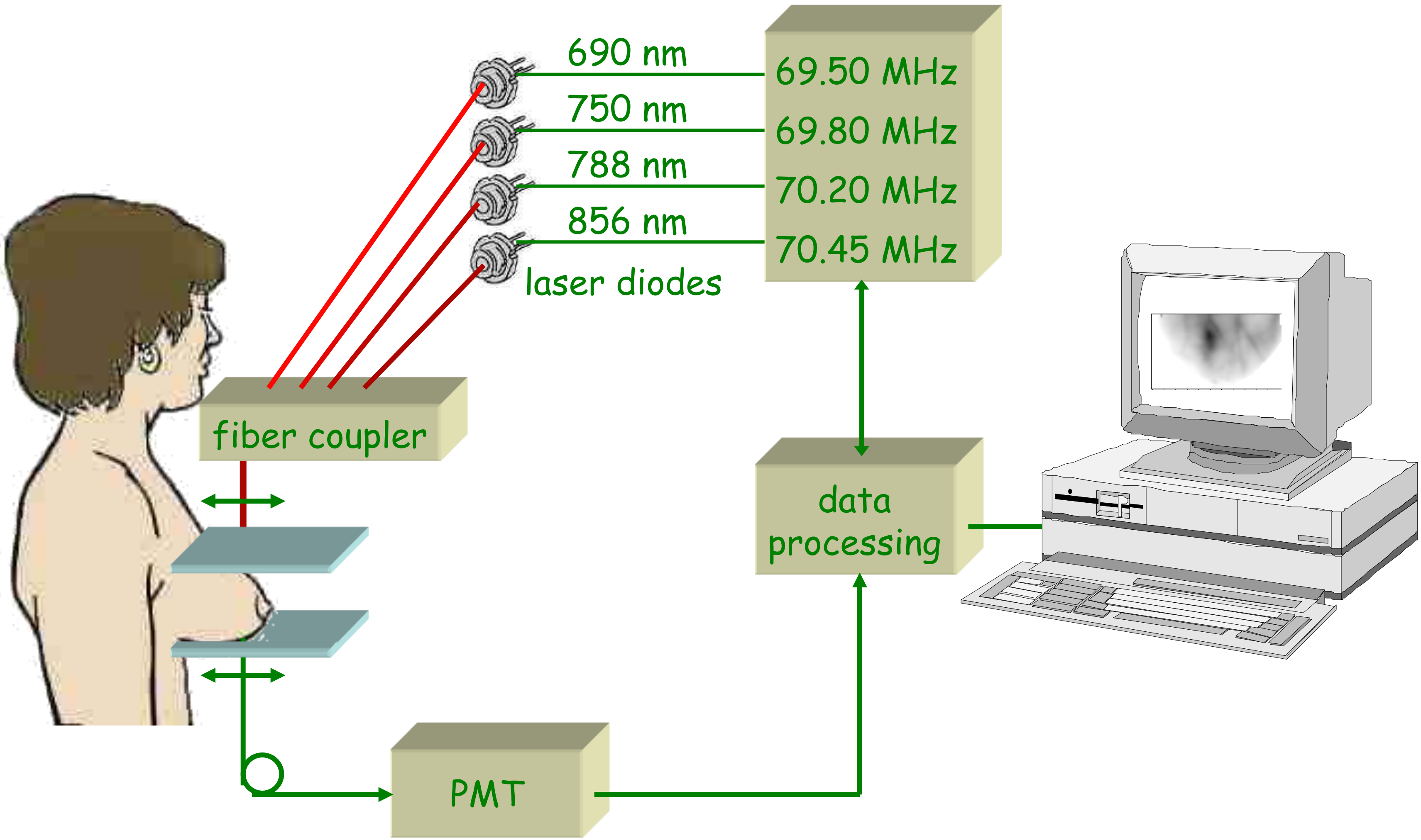

SIEMENS

SIEMENS

x-ray vs. optical mammography

invasive ductal cancer 3cm of diameter

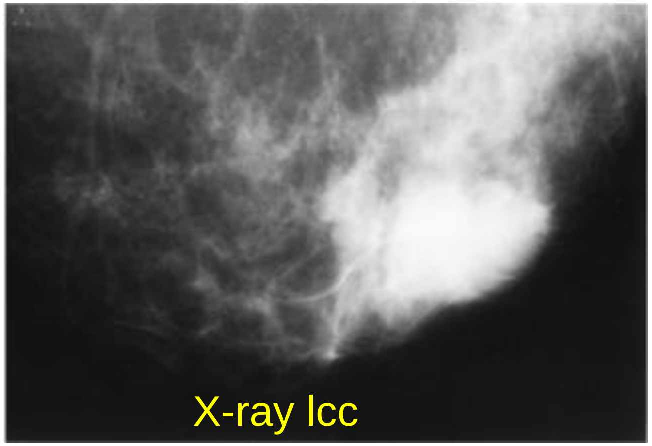

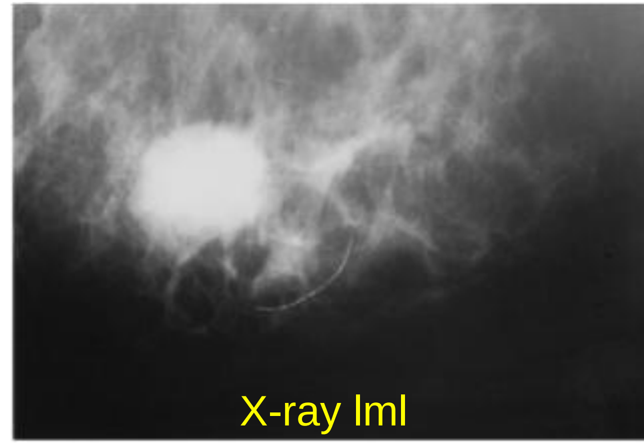

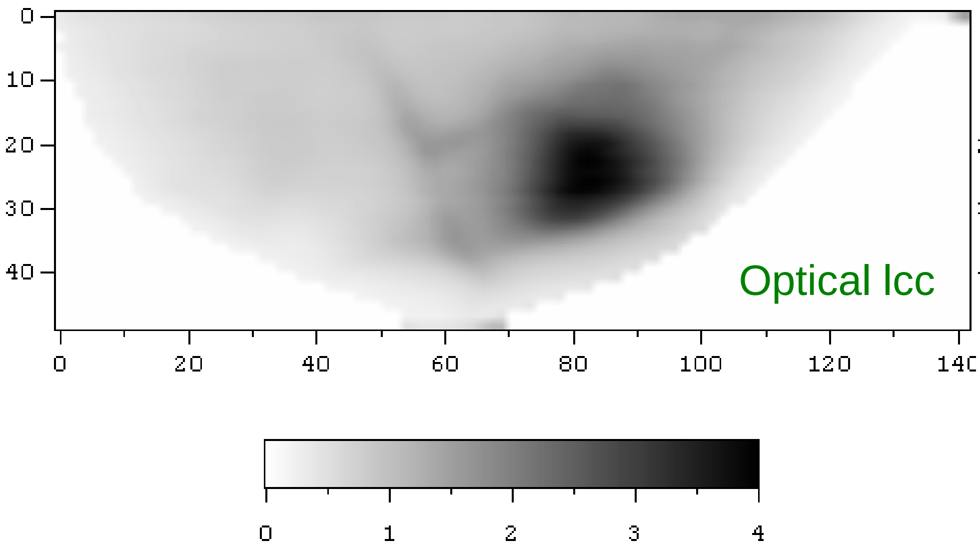

N @830 nm LCC

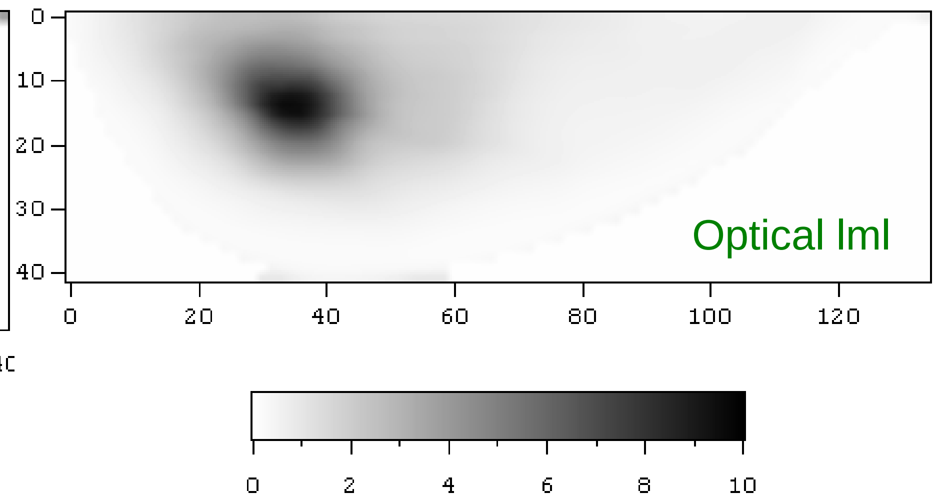

N @830 nm LML

P2-C30L

Franceschini *et al.*, Proc. Natl. Acad. Sci. USA **94**, 6468-6473 (1997)

Oxygenation Index images from multi-wavelength optical mammograms

N" images at four wavelengths

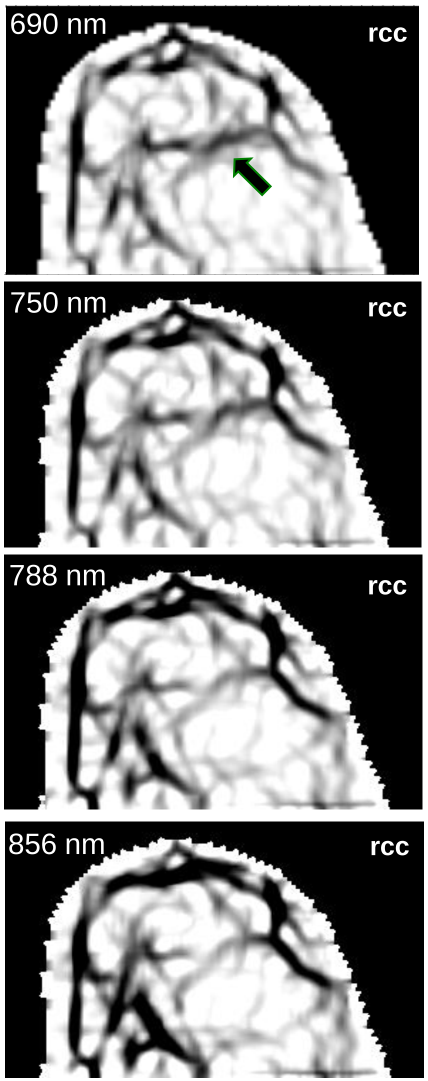

Oxygenation Index image

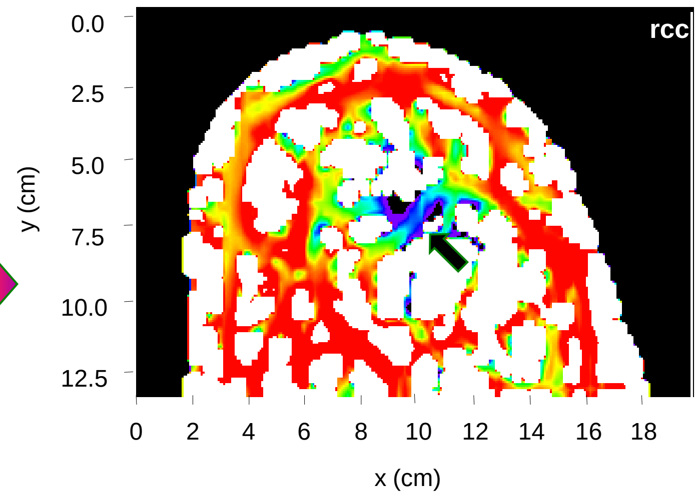

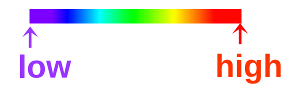

For pixels with a negative N":

$$\Delta[\mathrm{HbO_2}]^* = \frac{\left(\sum_i N''(\lambda_i)\varepsilon_{\mathrm{HbO2}}(\lambda_i)\right)\left(\sum_i \varepsilon^2_{\mathrm{Hb}}(\lambda_i)\right) - \left(\sum_i N''(\lambda_i)\varepsilon_{\mathrm{Hb}}(\lambda_i)\right)\left(\sum_i \varepsilon_{\mathrm{HbO2}}(\lambda_i)\varepsilon_{\mathrm{Hb}}(\lambda_i)\right)}{\left(\sum_i \varepsilon^2_{\mathrm{HbO2}}(\lambda_i)\right)\left(\sum_i \varepsilon^2_{\mathrm{Hb}}(\lambda_i)\right) - \left(\sum_i \varepsilon_{\mathrm{HbO2}}(\lambda_i)\varepsilon_{\mathrm{Hb}}(\lambda_i)\right)^2}$$

$$\Delta[\mathrm{Hb}]^* = \frac{\left(\sum_i N''(\lambda_i)\varepsilon_{\mathrm{Hb}}(\lambda_i)\right)\left(\sum_i \varepsilon^2_{\mathrm{HbO2}}(\lambda_i)\right) - \left(\sum_i N''(\lambda_i)\varepsilon_{\mathrm{HbO2}}(\lambda_i)\right)\left(\sum_i \varepsilon_{\mathrm{HbO2}}(\lambda_i)\varepsilon_{\mathrm{Hb}}(\lambda_i)\right)}{\left(\sum_i \varepsilon^2_{\mathrm{HbO2}}(\lambda_i)\right)\left(\sum_i \varepsilon^2_{\mathrm{Hb}}(\lambda_i)\right) - \left(\sum_i \varepsilon_{\mathrm{HbO2}}(\lambda_i)\varepsilon_{\mathrm{Hb}}(\lambda_i)\right)^2}$$

$$\text{Oxygenation Index} = \frac{\Delta[\mathrm{HbO_2}]^*}{\Delta[\mathrm{HbO_2}]^* + \Delta[\mathrm{Hb}]^*}$$

[S. Fantini *et al.*, Proc. SPIE **4955**, 183 (2003).]

Patient Number 215, 53 y.o.
3.0 cm invasive ductal carcinoma, left breast

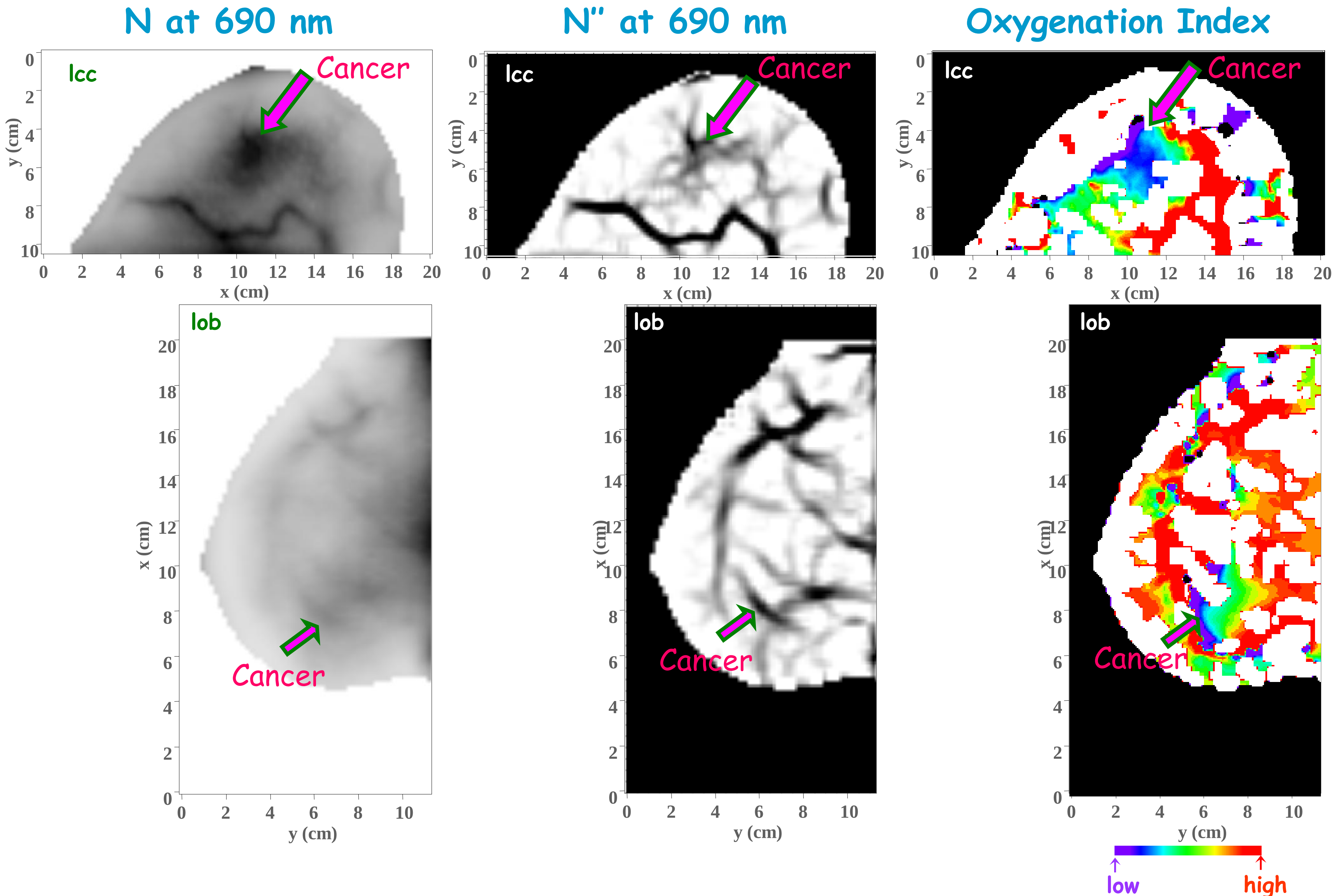

A more challenging case:
Cancer size < 0.5 cm

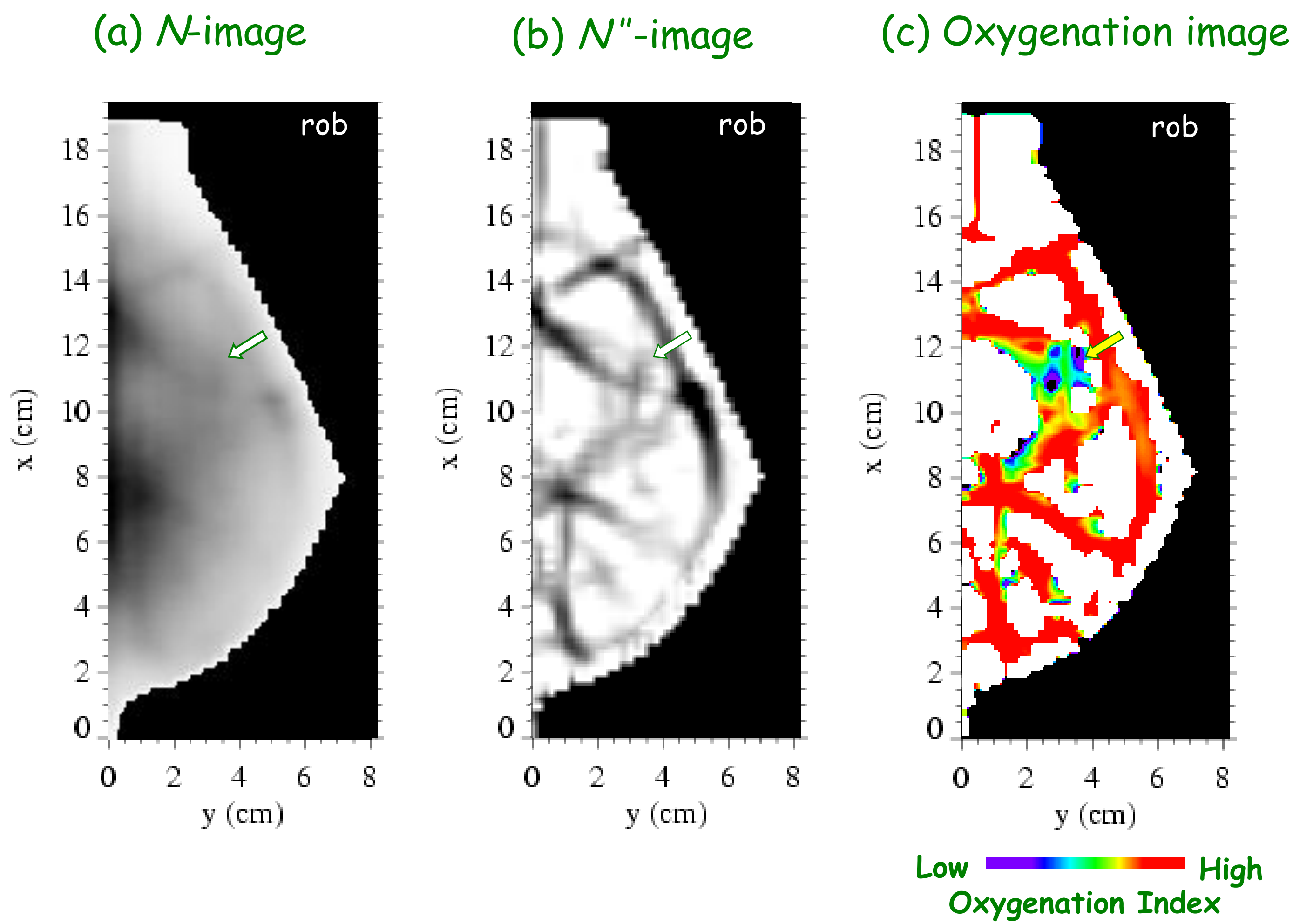

OPTICAL IMAGING OF THE BRAIN

The basic approach to optical imaging of the brain

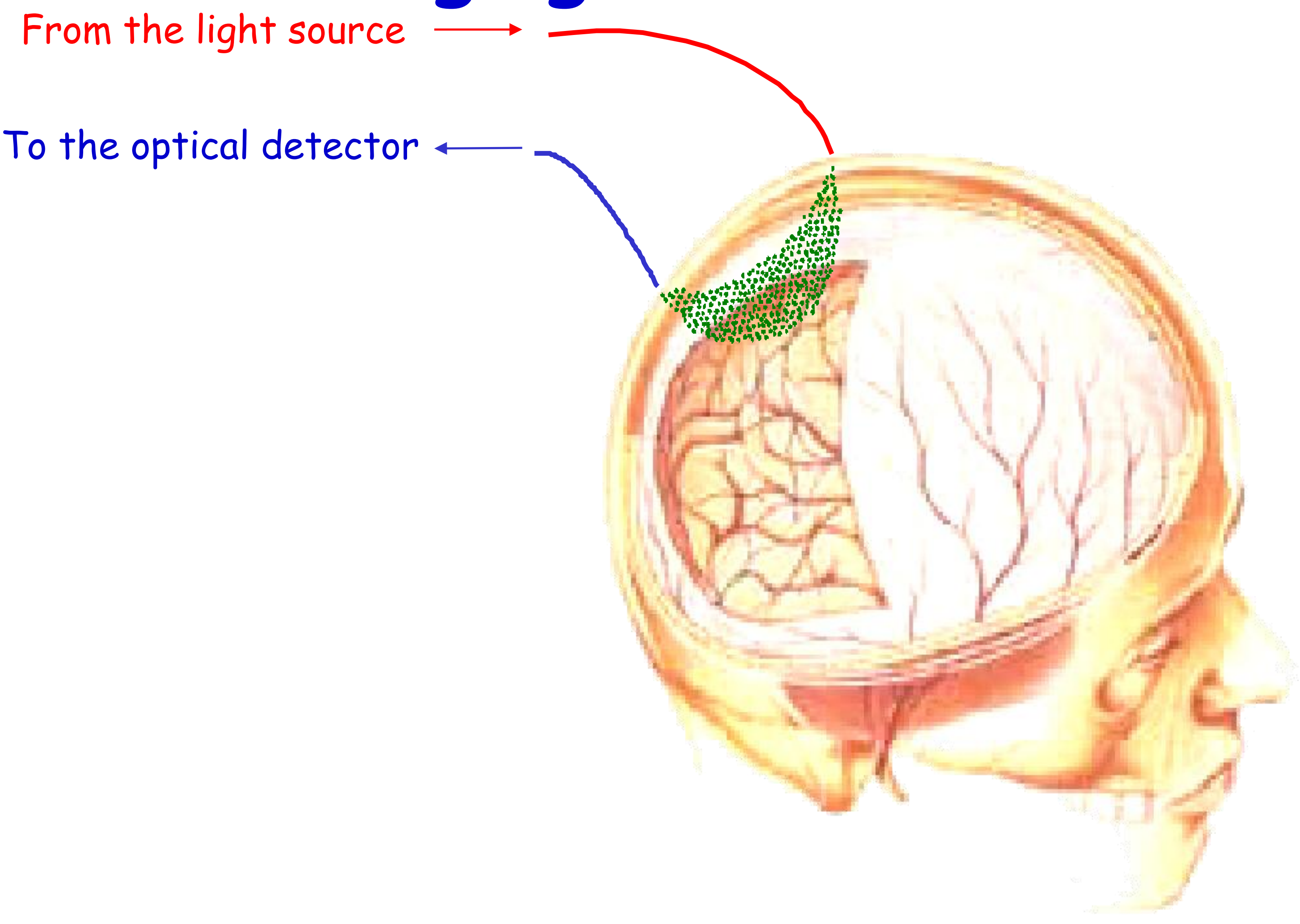

Bilateral optical imaging of the brain

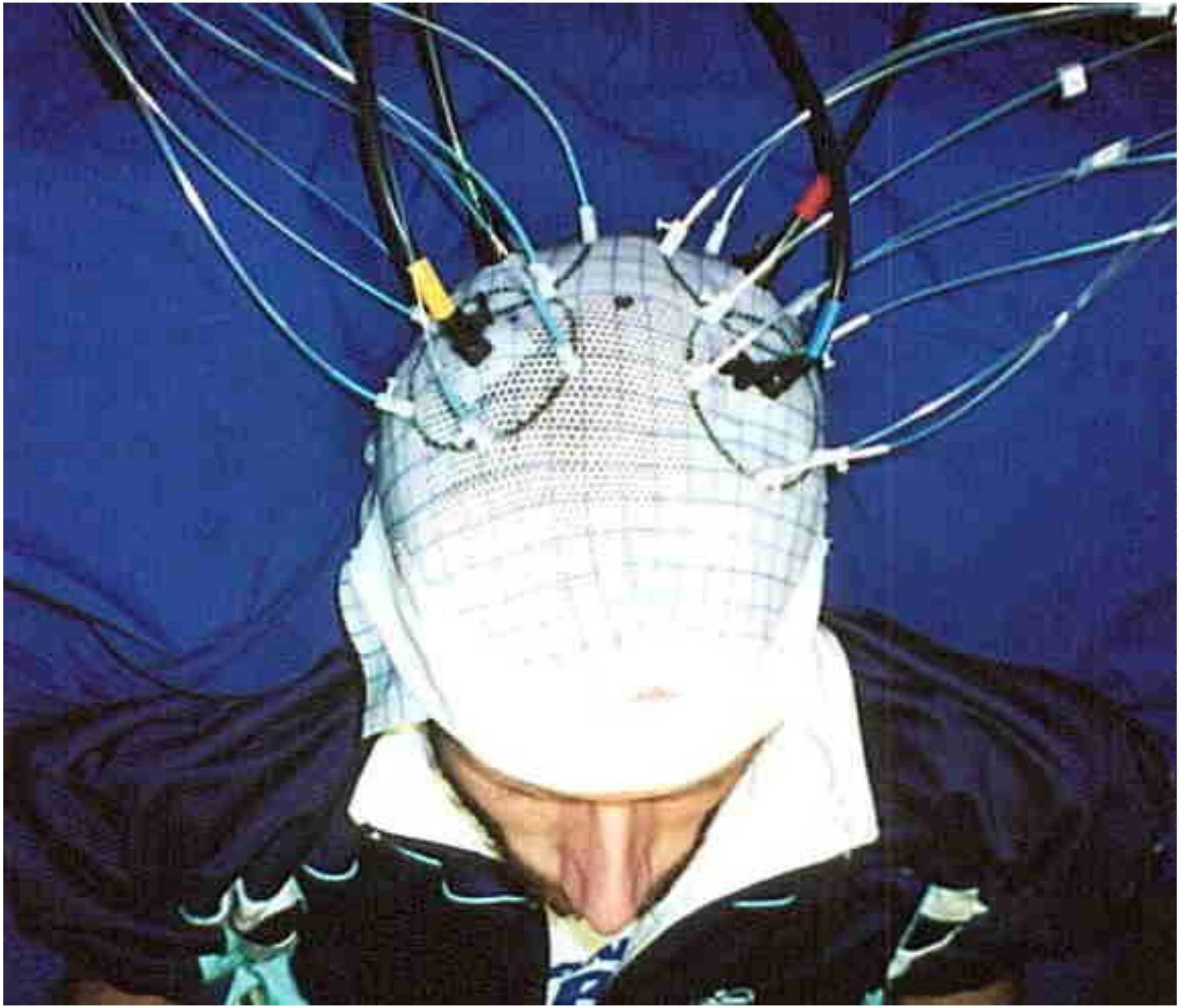

NIRS-fMRI compatible helmet

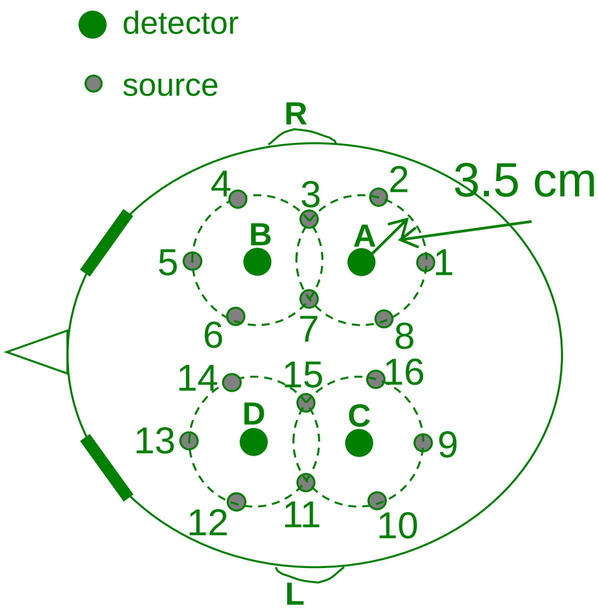

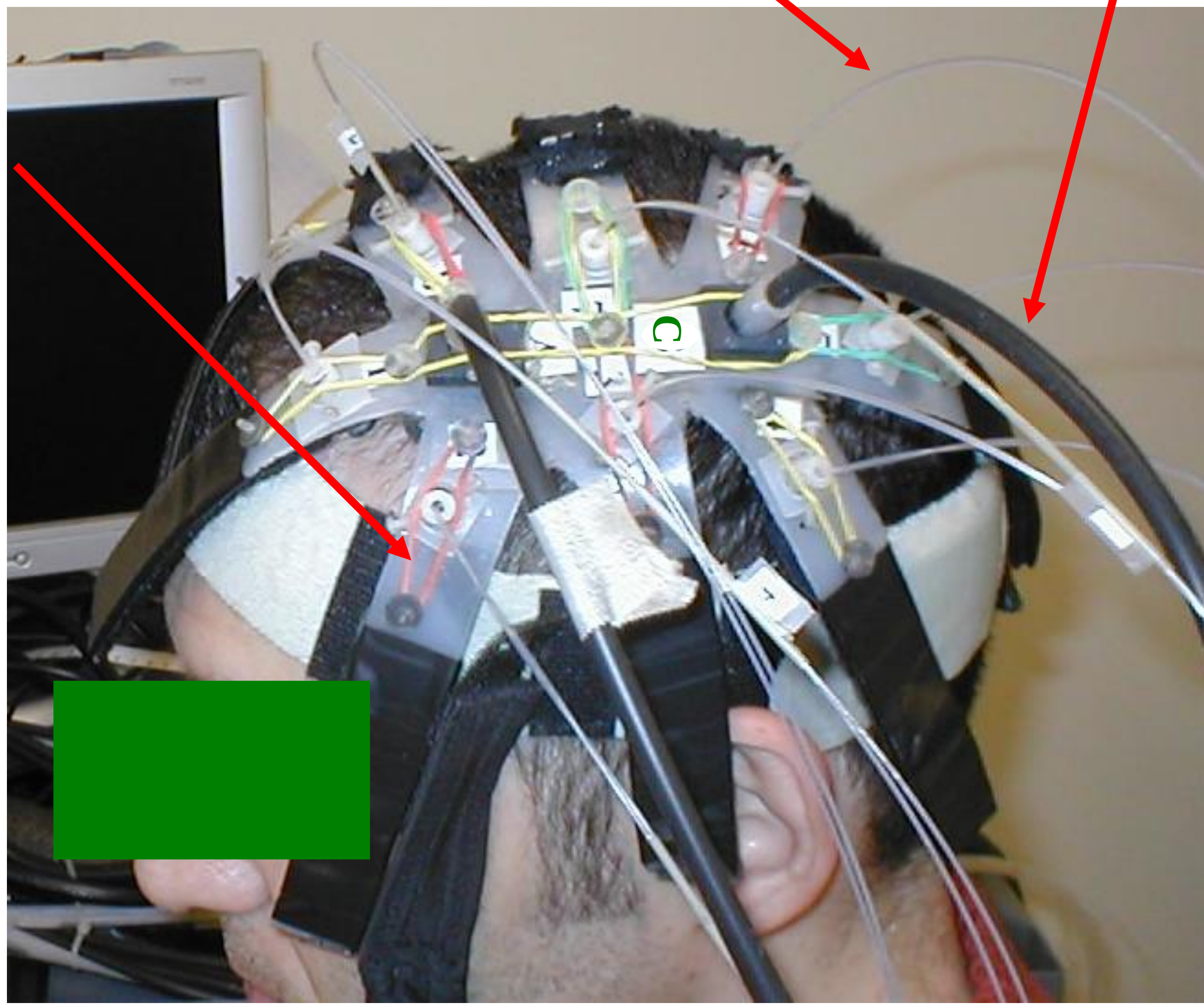

“Minority report,” year: 2054

Right hand tapping

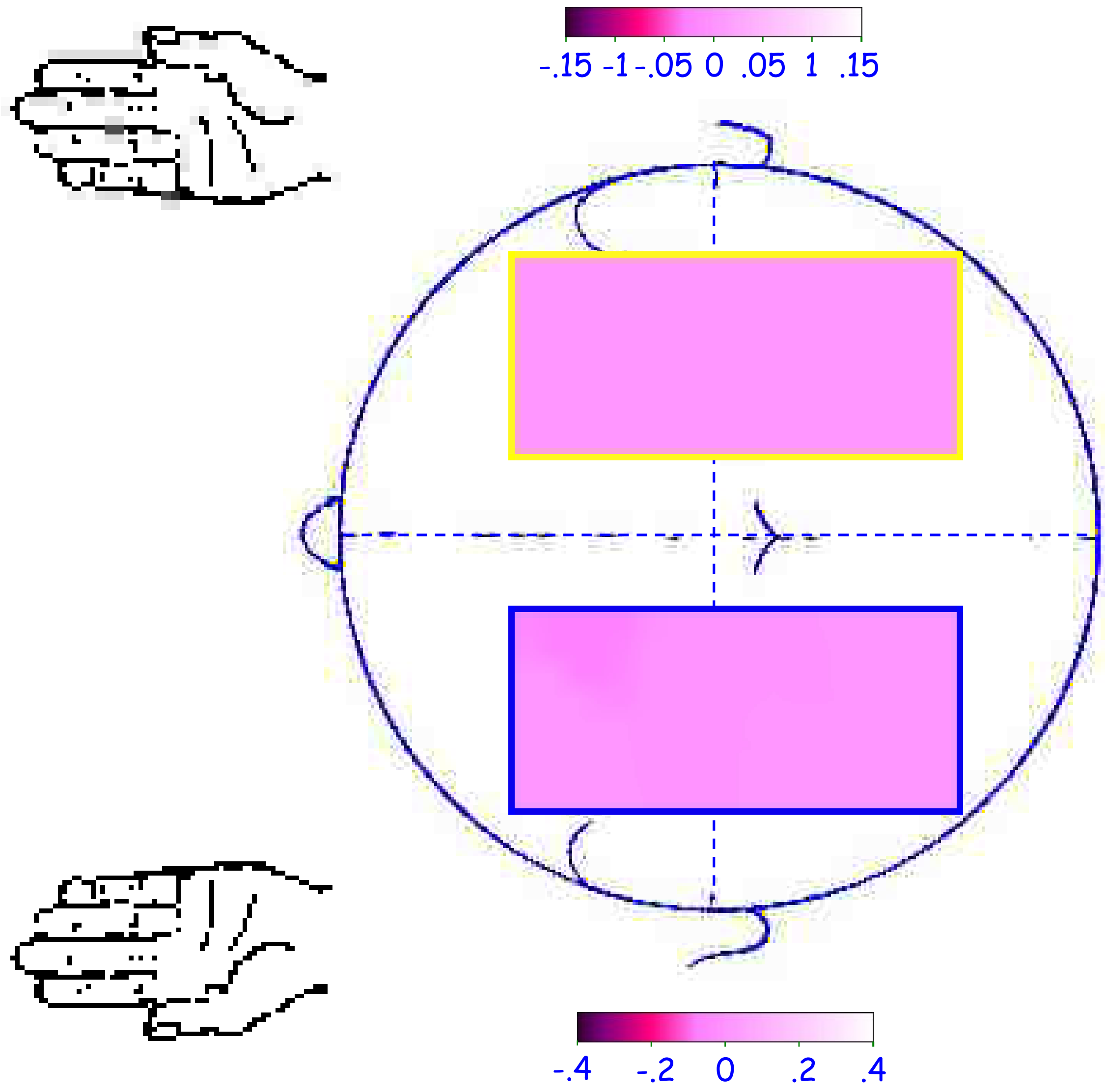

Δdeoxy-hemoglobing conc.(μM)

Right hand tapping

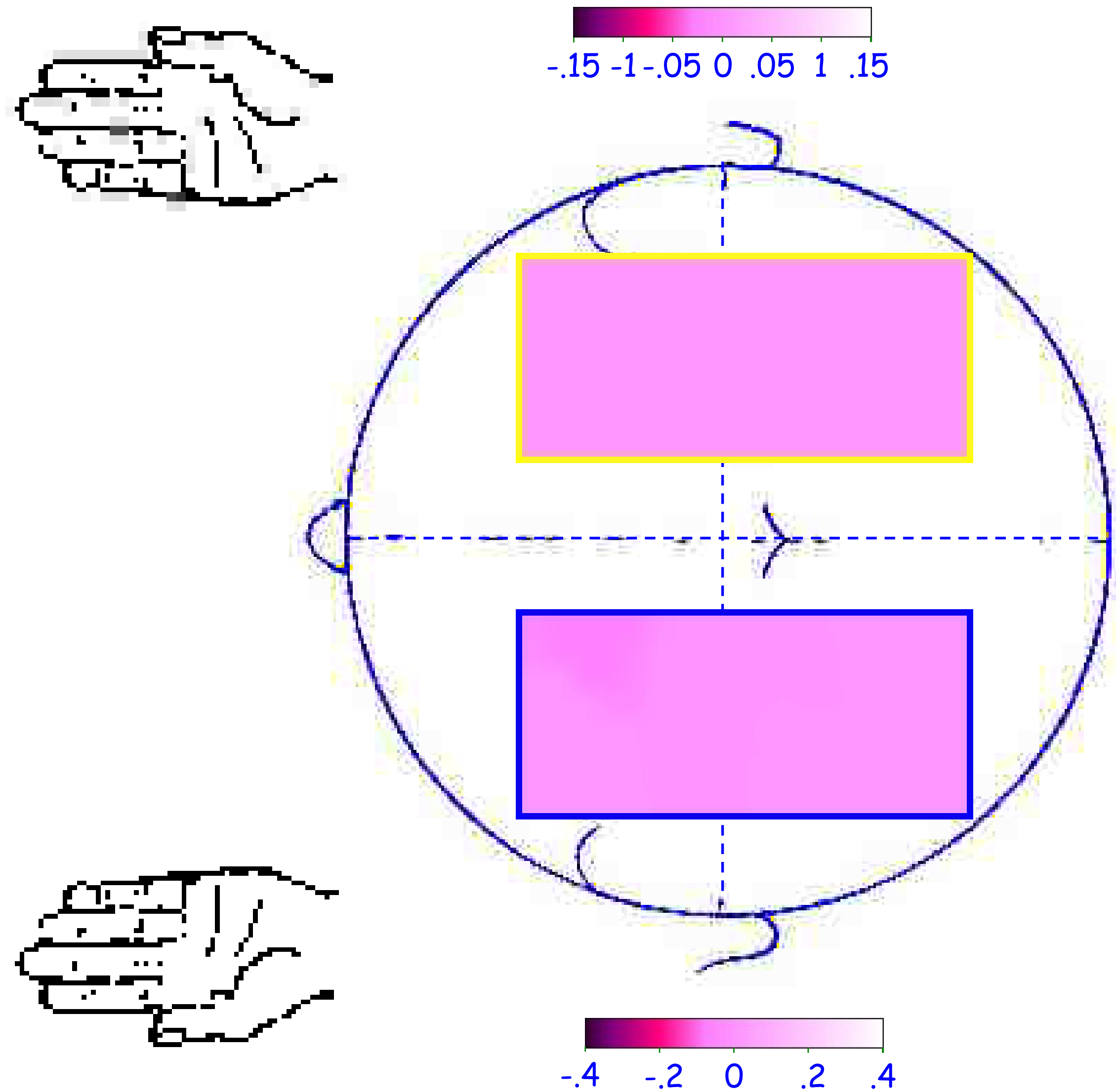

Δdeoxy-hemoglobing conc.(μM)

left hand tapping

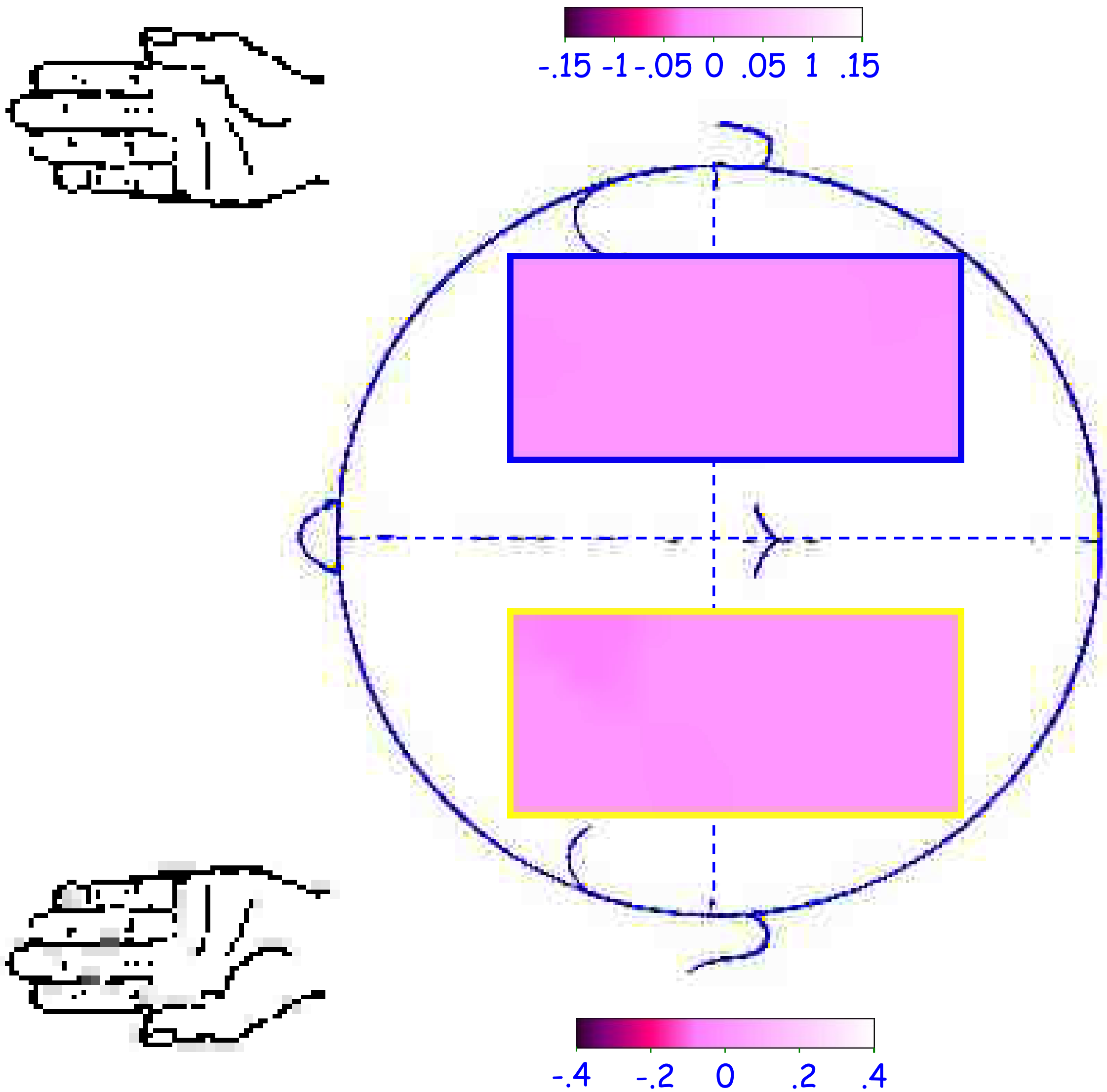

Δdeoxy-hemoglobing conc.(μM)

left hand tapping

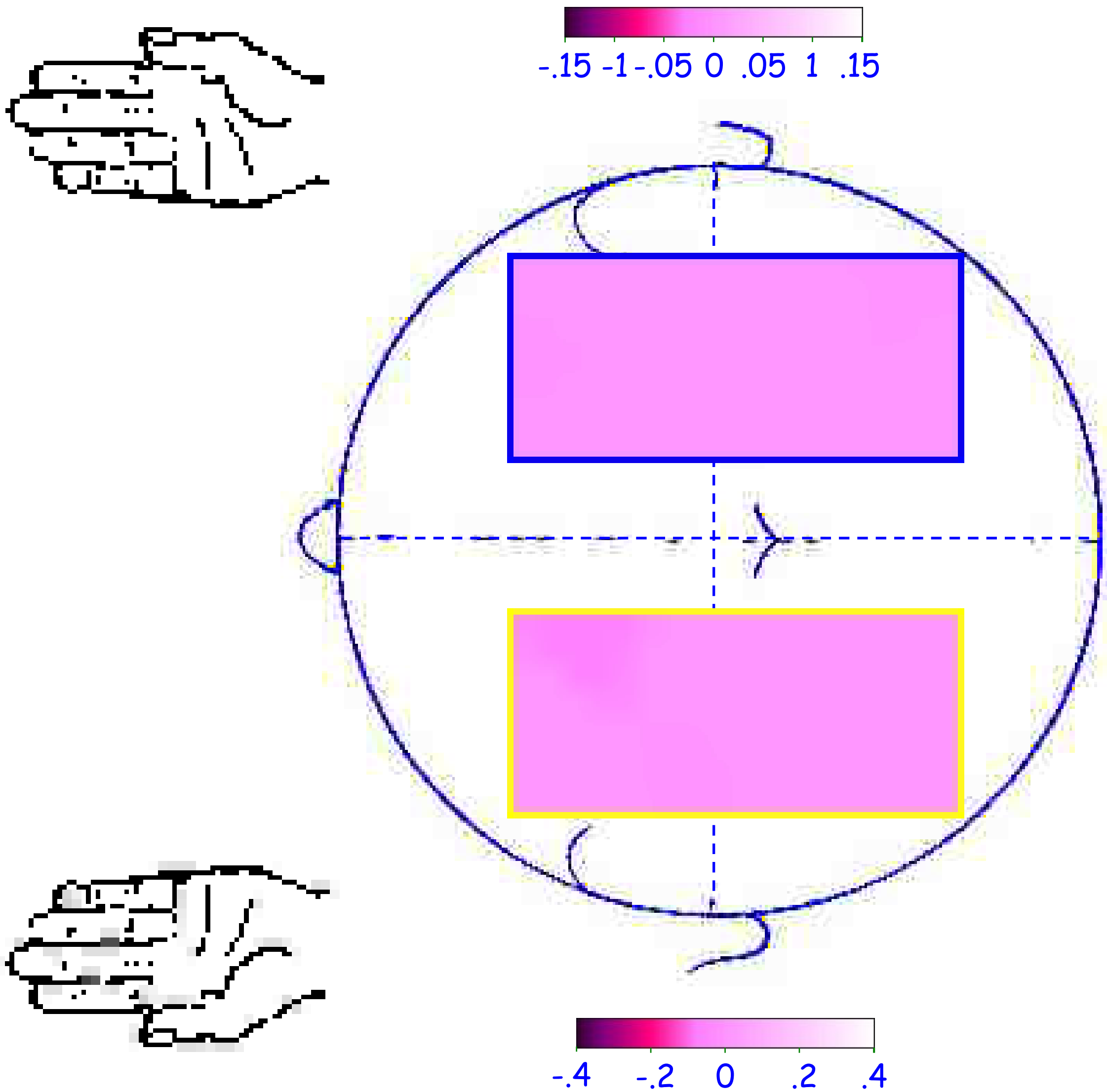

Δdeoxy-hemoglobing conc.(μM)

Hemodynamic response to brain activation

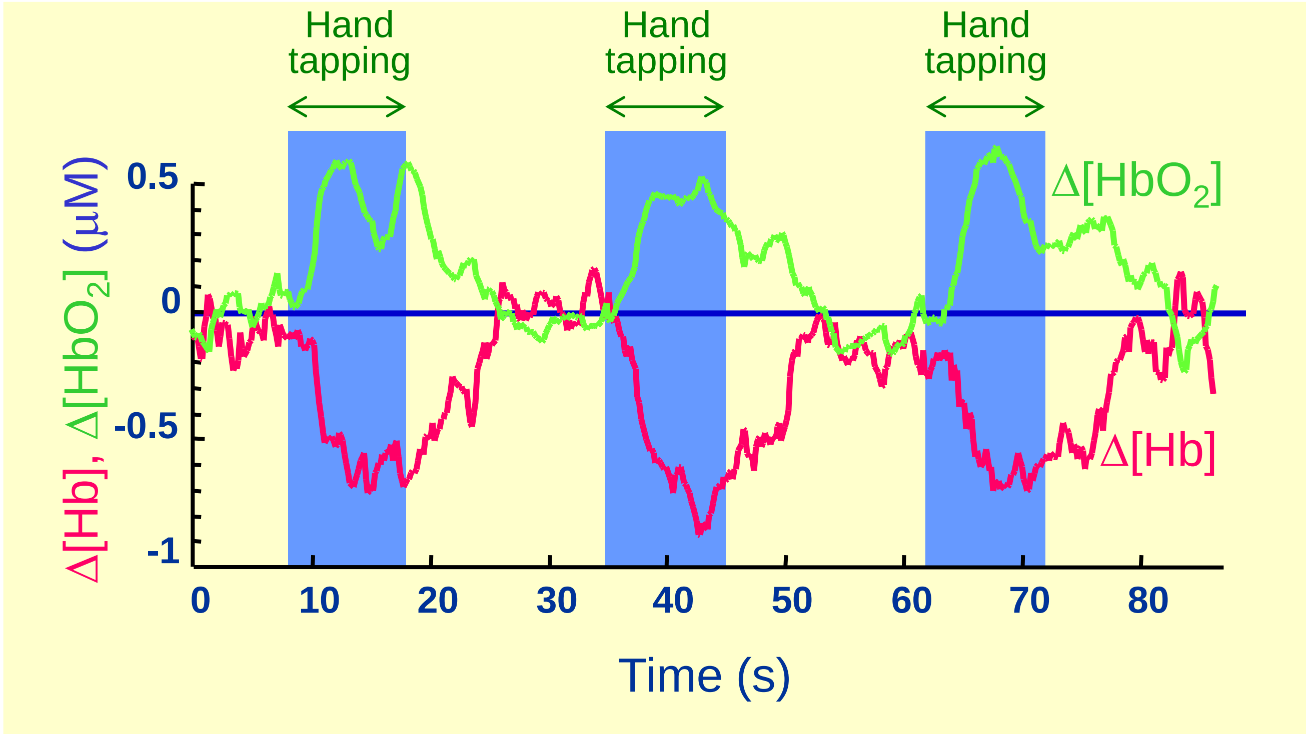

$$\Delta[\mathrm{Hb}]^{(\mathrm{tissue})} = [\mathrm{HbT}]^{(\mathrm{blood})}\frac{V_{\mathrm{bv}}}{V}\left[1-\mathrm{SO}_2\Big|_0^{(\mathrm{blood})}\frac{c^{(\mathrm{blood})}}{\alpha_{\dot{\mathrm{O}}_2}L_{\mathrm{bv}}}\left(1-e^{-\frac{\alpha_{\dot{\mathrm{O}}_2}L_{\mathrm{bv}}}{c^{(\mathrm{blood})}}}\right)\right]\left(\frac{\Delta[\mathrm{HbT}]^{(\mathrm{blood})}}{[\mathrm{HbT}]^{(\mathrm{blood})}}+\frac{\Delta\sigma_{\mathrm{bv}}}{\sigma_{\mathrm{bv}}}\right)$$

$$+\mathrm{SO}_2\Big|_0^{(\mathrm{blood})}[\mathrm{HbT}]^{(\mathrm{blood})}\frac{c^{(\mathrm{blood})}\sigma_{\mathrm{bv}}}{\alpha_{\dot{\mathrm{O}}_2}V}\left(1-e^{-\frac{\alpha_{\dot{\mathrm{O}}_2}L_{\mathrm{bv}}}{c^{(\mathrm{blood})}}}\right)\left(-\frac{\Delta\mathrm{SO}_2\Big|_0^{(\mathrm{blood})}}{\mathrm{SO}_2\Big|_0^{(\mathrm{blood})}}\right)$$

$$+\mathrm{SO}_2\Big|_0^{(\mathrm{blood})}[\mathrm{HbT}]^{(\mathrm{blood})}\frac{c^{(\mathrm{blood})}\sigma_{\mathrm{bv}}}{\alpha_{\dot{\mathrm{O}}_2}V}\left[1-e^{-\frac{\alpha_{\dot{\mathrm{O}}_2}L_{\mathrm{bv}}}{c^{(\mathrm{blood})}}}\left(\frac{\alpha_{\dot{\mathrm{O}}_2}L_{\mathrm{bv}}}{c^{(\mathrm{blood})}}+1\right)\right]\left(\frac{\Delta\alpha_{\dot{\mathrm{O}}_2}}{\alpha_{\dot{\mathrm{O}}_2}}-\frac{\Delta c^{(\mathrm{blood})}}{c^{(\mathrm{blood})}}\right),$$

[S. Fantini, Phys. Med. Biol. **47**, N249 (2002)]

Concurrent fMRI and fNIRS

Comparison of BOLD and NIRS mapping

Right hand tapping

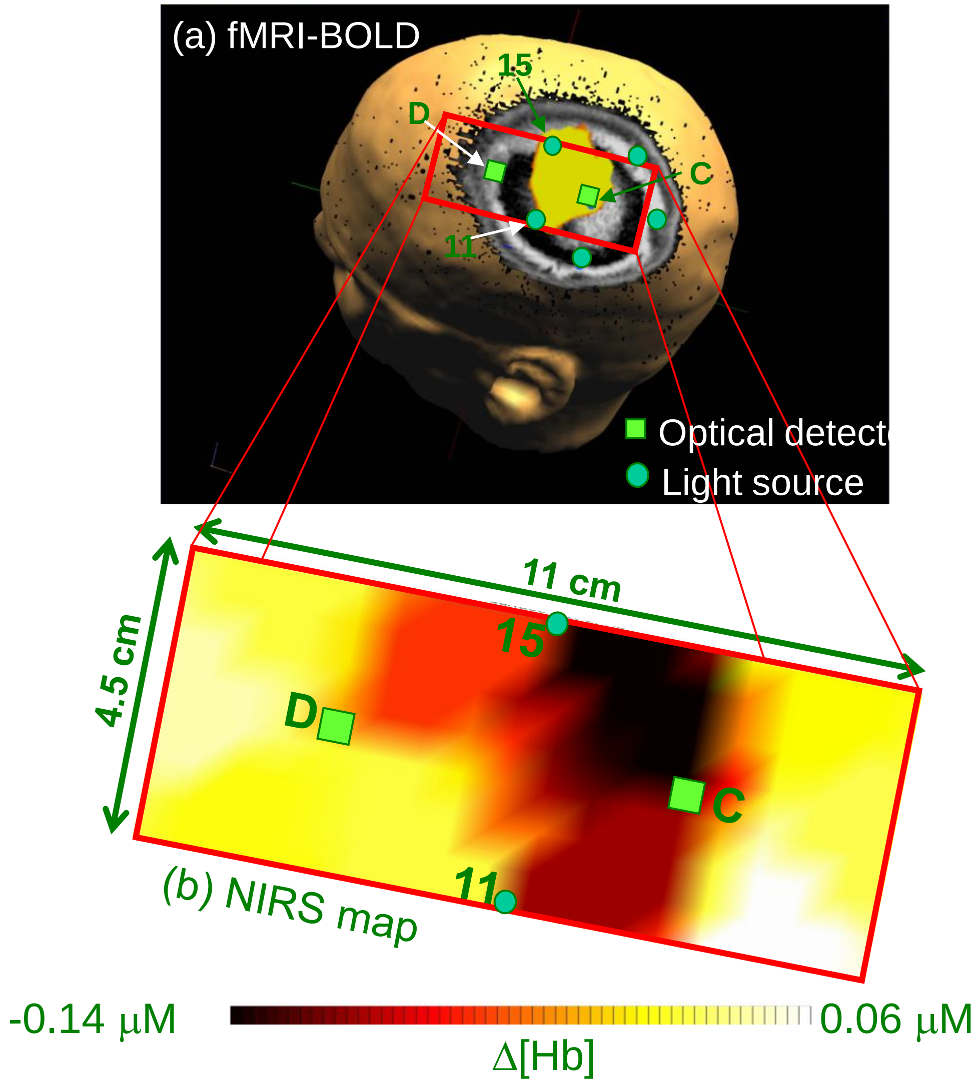

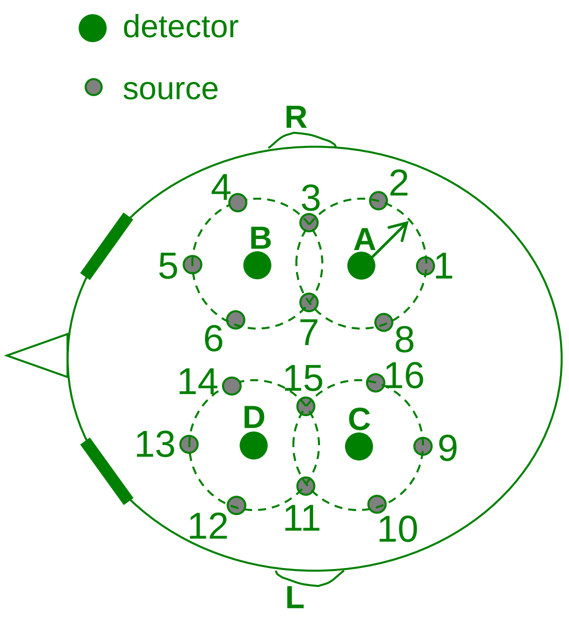

Weighted average of BOLD signal according to photon-hitting density function

k = 0.3 mm^{-1}

(μ_a=0.020 mm^{-1}, μ_s'=1.5 mm^{-1})

Fig.5

$BOLD_{PMA}$ and NIRS maps (Right side): Comparison at t = 6 s

Left hand tapping

NIRS:

Δ[Hb]

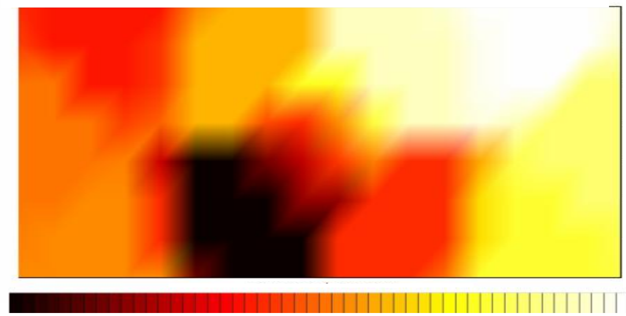

Δ[HbO]

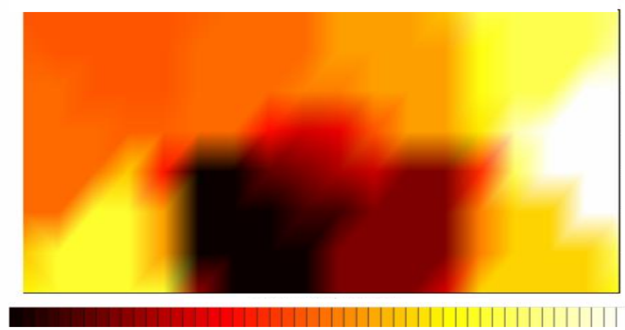

fMRI: $BOLD_{PMA}$

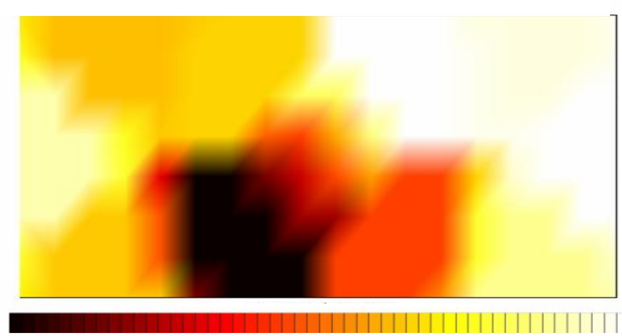

Comparison of BOLD$_{PMA}$ and NIRS Signals: Temporal correlation

Left hand tapping

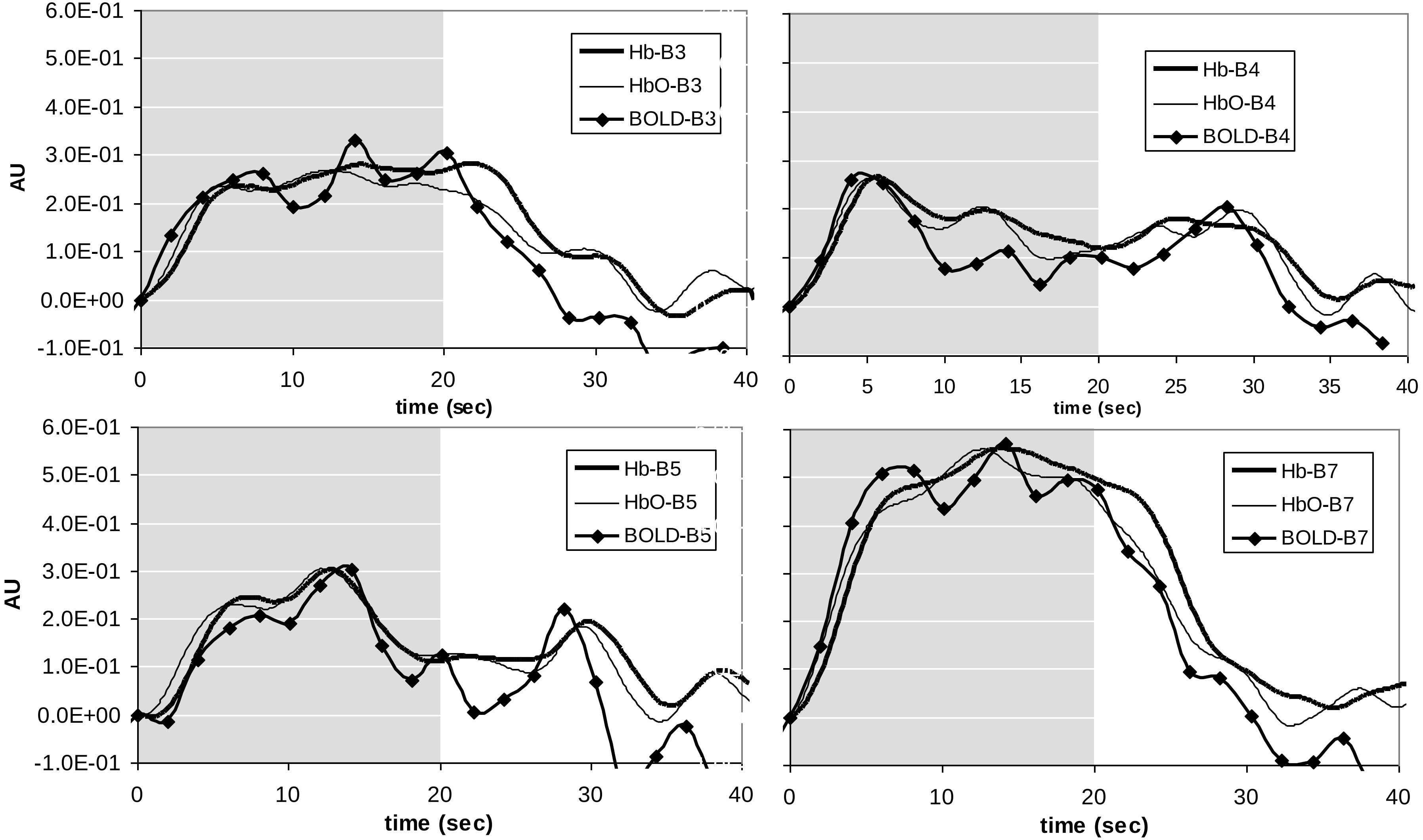

Conclusioni

La spettroscopia nel vicino infrarosso e’ una tecnica non invasiva per applicazioni in campo diagnostico e di ricerca:

- **Ossimetria tissutale quantitativa**
- **Rivelazione/monitoraggio del tumore della mammella**
- **Studio in tempo reale della funzionalita’ cerebrale**

Near-infrared spectroscopy group @ Tufts University

- Yang Yu, PhD Student
- Sergio Fantini, Prof.
- Angelo Sassaroli, Res. Assoc.
- Yunjie Tong, PhD Student
- Jeff Martin, MS/MD Student
- Debbie Chen, PhD Student
- Ning Liu, PhD Student

Acknowledgments:

NSF-CAREER: BES93840

NIH-NIDA: DA14178

NIH-NCI: CA95885